ETH zürich

ETH Library

Adaptation to local climate in multi-trait space: evidence from silver fir (Abies alba Mill.) populations across a heterogeneous environment

Journal Article

Author(s):
Csilléry, Katalin; Ovaskainen, Otso; Sperisen, Christoph; Buchmann, Nina; Widmer, Alex; Gugerli, Felix

Publication date:
2020

Permanent link:
https://doi.org/10.3929/ethz-b-000383389

Rights / license:
In Copyright - Non-Commercial Use Permitted

Originally published in:
Heredity 124, https://doi.org/10.1038/s41437-019-0240-0

This page was generated automatically upon download from the ETH Zurich Research Collection.
For more information, please consult the Terms of use.

Title: Adaptation to local climate in multi-trait space: evidence from silver fir (*Abies alba* Mill.) populations across a heterogeneous environment

Authors: Katalin Csilléry[1,2,*], Otso Ovaskainen[3,4], Christoph Sperisen[2], Nina Buchmann[5], Alex Widmer[6], Felix Gugerli[2]

Addresses:
[1] Center for Adaptation to a Changing Environment, Institute of Integrative Biology, ETH Zurich, Zurich, Switzerland
[2] Swiss Federal Research Institute WSL, Birmensdorf, Switzerland
[3] Faculty of Biological and Environmental Sciences, University of Helsinki, Helsinki, Finland
[4] Centre for Biodiversity Dynamics, Department of Biology, Norwegian University of Science and Technology, Trondheim, Norway
[5] Institute of Agricultural Sciences, ETH Zurich, Zurich, Switzerland
[6] Institute of Integrative Biology, ETH Zurich, Zurich, Switzerland
[*]**Current address:** Department of Evolutionary Biology and Environmental Studies, University of Zurich, Zurich, Switzerland

Corresponding author: Katalin Csilléry
Department of Evolutionary Biology and Environmental Studies, University of Zurich
Biodiversity & Conservation Biology, Swiss Federal Research Institute WSL
Zürcherstrasse 111
8903 Birmensdorf, Switzerland
Email: katalin.csillery@uzh.ch or kati.csillery@gmail.com
Tel: +41 44 739 25 23
Fax: +41 44 739 22 15

Running title: Adaptation across a heterogeneous environment in silver fir

Word count: 7124

Abstract

Heterogeneous environments, such as mountainous landscapes, create spatially varying selection pressure that potentially affects several traits simultaneously across different life stages, yet little is known about the general patterns and drivers of adaptation in such complex settings. We studied silver fir (*Abies alba* Mill.) populations across Switzerland and characterized their mountainous landscape using downscaled historical climate data. We sampled 387 trees from 19 populations and genotyped them at 374 single-nucleotide polymorphisms (SNPs) to estimate their demographic distances. Seedling morphology, growth and phenology traits were recorded in a common garden, and a proxy for water use efficiency was estimated for adult trees. We tested whether populations have more strongly diverged at quantitative traits than expected based on genetic drift alone in a multi-trait framework, and identified potential environmental drivers of selection. We found two main responses to selection: (i) populations from warmer and more thermally stable locations have evolved towards a taller stature, and (ii) the growth timing of populations evolved towards two extreme strategies, "start early and grow slowly" or "start late and grow fast", driven by precipitation seasonality. Populations following the "start early and grow slowly" strategy had higher water use efficiency and came from inner Alpine valleys characterized by pronounced summer droughts. Our results suggest that contrasting adaptive life-history strategies exist in silver fir across different life stages (seedling to adult), and that some of the characterized populations may provide suitable seed sources for tree growth under future climatic conditions.

Keywords:

selection, demography, quantitative trait, ontogeny, life-history, stable carbon isotopes

Introduction

Phenotypic differences between populations may reflect neutral, adaptive, and/or plastic processes (Kawecki & Ebert, 2004). Neutral processes often lead to phenotypic differentiation between populations at the species' range edges, where populations are small and isolated (*e.g.* Hampe & Petit, 2005, Kawecki, 2008). The relative importance of adaptation and plasticity ultimately depends on the degree of environmental heterogeneity and the dispersal ability of the species (Via & Lande, 1985, Sultan & Spencer, 2002, Chevin & Lande, 2010, Polechova, 2018). Local adaptation is likely to establish when the spatial scale of environmental variation is greater than the dispersal ability of the species, while plasticity is likely to be favoured with a fine-scale environmental variability and/or in the presence of long-distance gene flow.

Forest trees have large effective population sizes, species ranges that span large spatial scales, a long-life span and a predominantly outcrossing mode of reproduction (Petit & Hampe, 2006). Long-distance gene flow is also common in forest trees and its role in adaptation has been recognized (Kremer *et al.*, 2012). These characteristics largely favour plasticity, which has been illustrated by multi-site common garden trials, for example for growth (*e.g.* Rehfeldt *et al.*, 2002) or phenology (*e.g.* Vitasse *et al.*, 2010, De Kort *et al.*, 2016); see further references in Kremer *et al.* (2012). Nevertheless, local adaptation is also common in forest trees, with ample evidence for adaptive divergence along continuous environmental clines, such as those created by latitude or distance to the sea in the boreal zone, or altitudinal gradients in the temperate zone (Savolainen *et al.*, 2007,

Alberto *et al.*, 2011, Lind *et al.*, 2018).

While adaptation has been extensively studied along environmental gradients, much less is known about its general patterns and drivers in heterogeneous environments. Indeed, populations across heterogeneous landscapes may display rapid and often non-predictable changes in genetic diversity and trait divergence (Yeaman & Jarvis, 2006). Mountainous regions of the Northern Hemisphere often create such heterogeneous landscapes for many species. Here, post-glacial recolonization not only traced the climatic niche, but was also constrained by topography, creating complex patterns in species distributions and demography (Hewitt, 1999). Environmental drivers of adaptation in mountain ranges can go undetected with coarse-scale climate data (*e.g.* Austin & Van Niel, 2011, Ruosch *et al.*, 2016). The development of many fine–scale environmental data sets provides new opportunities to study adaptation across mountainous landscapes (*e.g.* Karger *et al.*, 2017, Hengl *et al.*, 2017). It is also increasingly recognized that spatial heterogeneity in climate in mountainous landscapes represents an important spatial buffer in response to climate change (*e.g.* Ackerly *et al.*, 2010).

The phenotypic signature of spatially varying selection across populations can be assessed using Q_{ST}, a measure of genetic differentiation between populations (Whitlock, 2008). Comparing Q_{ST} with divergence at neutral genetic markers (F_{ST}) provides a means for identifying locally adapted populations (Whitlock, 2008, Whitlock & Guillaume, 2009). In principle, a comparison of Q_{ST} to F_{ST} controls for demography, but insufficiently so, because the complex history of potentially numerous populations cannot be adequately represented by F_{ST}. This issue has been

widely recognized and alternative solutions have been suggested (*e.g.* Chenoweth & Blows, 2008, Martin *et al.*, 2008). The most complete approach has been proposed by Ovaskainen *et al.* (2011), which uses a statistically more powerful and biologically more meaningful null hypothesis: it accounts for the neutral demographic distances among all populations to derive a null expectation of trait divergence (see applications in (*e.g.* De Kort *et al.*, 2016, Schäfer *et al.*, 2018)). Furthermore, most past studies assessed traits in isolation from each other and focus on traits that are likely affected by the studied environmental gradient. The method of Ovaskainen *et al.* (2011) can be used to assess adaptive divergence on multiple traits at a time, thus potentially identify adaptive life-history strategies.

Most evidence for adaptive divergence in forest trees comes from seedling traits measured in common garden experiments. Although multiple seedling traits can be used to identify adaptive life-history strategies, it is difficult to assess if results are transferable to natural populations (*e.g.* Neale & Kremer, 2011). Indeed, trees have a long life span with two characteristic life-history stages, seedling and adult, where different selection pressures and physiological processes are operating (Petit & Hampe, 2006). Connecting these two life stages is essential because seedling mortality has the largest impacts on the structure and function of future forests, while the death of big trees causes the longest lasting carbon losses (McDowell *et al.*, 2013). Tree breeders have long known that seed or seedling traits are often poor predictors of adult traits in field conditions (*e.g.* Resende *et al.*, 2012), with some exceptions, e.g. wood traits (Gaspar *et al.*, 2008) or seed size in pines (Zas & Sampedro, 2015). Measures of adult

growth traits *in-situ* may also be uninformative when they are affected by management practices and competition, even if this effect is less pronounced for shade-tolerant species, such as silver fir (Kunstler *et al.*, 2011). In contrast, carbon stable isotope discrimination, δ^{13}C, may represent a suitable trait for adult trees. δ^{13}C is related to the intrinsic water-use efficiency, a measure of relative water loss per molecule carbon acquired in the leaf, and has been advocated as a proxy for drought tolerance (Farquhar *et al.*, 1989). In vascular plants, δ^{13}C is to a large extent genetically determined (Dawson *et al.*, 2002), and several important quantitative trait loci (QTL) have been identified in forest trees (Brendel *et al.*, 2002, 2008). Further, for example, in *Picea mariana*, δ^{13}C was highly negatively genetically correlated to growth, while being less environmentally sensitive than growth, thus the authors suggested this trait for indirect selection for growth (Johnsen *et al.*, 1999). Overall, δ^{13}C is one of the key traits for understanding the genetics of drought tolerance (Moran *et al.*, 2017).

Here, we study adaptive divergence patterns in populations of silver fir (*Abies alba* Mill.) across a highly heterogeneous mountainous landscape. We asked whether populations have developed adaptive life-history strategies in response to local climatic conditions that are consistently present from the seedling to adult stage, while controlling for demographic distances between populations. Seedling morphology, growth and phenology were recorded in a common garden on half-sib families. We hypothesized that traits most likely do not evolve independently, thus we used a multi-trait quantitative genetic approach to identify correlated responses to selection. Adult δ^{13}C was measured *in-situ* on unrelated

individuals, and was used to correlate the populations' mean water use efficiency in the field with the populations' mean life-history strategies in seedlings. We developed a set of fine spatial scale historical climate variables to identify potential drivers of locally adapted life-history strategies. Finally, we estimate the evolutionary potential in seedling quantitative traits to assess the future of silver fir populations in Switzerland.

Material and Methods

Study system

Silver fir is an ecologically and economically important European conifer. It can likely tolerate episodes of drought due to its deep rooting system (*e.g.* Lebourgeois *et al.*, 2013, Vitali *et al.*, 2017) and its high tolerance to bark beetle attack (Wermelinger, 2004). We selected 19 putatively autochthonous silver fir populations across a highly heterogeneous Alpine region across the Swiss Alps, Pre-Alps, Central Plateau and Jura Mountains (Fig. 1a, Supporting Information Fig. S1 and Table S1). The selection was based on various data sources, including the national register of seed stands (NKS, for autochthony/allochthony information), national forest inventory (NFI, for the distribution of silver fir and stand histories), the long-term forest ecosystem research (LWF), and after consulting forest experts. In 2009, seeds were collected from three trees, and in 2013 and 2016, needles were sampled from 19 to 22 adult trees per population (total of 387 trees), including the previously sampled trees. A minimum distance of 100m was

respected between the sampled trees to minimize the risk of collecting closely related trees (e.g. parent-offspring or sibs). Note that it is common practice to sample adult trees with only 20m (Mosca *et al.*, 2012) or 37m (Roschanski *et al.*, 2016) minimum distance for population samples.

Based on palynological evidence, it is likely that the Swiss range of silver fir was colonized from south to north after the Last Glacial Maximum. The species most likely reached the southern slopes of the Alps between 10 and 9 kyr BP and the northern slopes between 8 and 5 kyr BP (Van der Knaap *et al.*, 2005, Liepelt *et al.*, 2009, Ruosch *et al.*, 2016). Range-wide patterns of chloroplast and mitochondrial DNA variation (Liepelt *et al.*, 2002) and isozyme data (Burga & Hussendörfer, 2001) from extant silver fir populations suggest that the Swiss Alps were colonized from a single ancestral refugial population situated in the Central and/or Northern Apennines, even though the potential contribution of eastern refugial populations cannot be excluded.

Adult tree data

All adult trees were genotyped at 374 single-nucleotide polymorphism (SNP) loci originating from three different sources. Our aim was to estimate demographic distances between populations, so we attempted to select principally neutral markers. First, we used 220 out of 267 SNPs from Roschanski *et al.* (2016): we excluded the 25 SNPs that coded for non-synonymous mutations and 22 others where we had more than 10% missing data. Second, we selected 110 new putatively neutral SNPs from the transcriptome assembly of Roschanski *et al.* (2016), based on respective values of Tajima's D between 2 and -2 and dN/dS between 0.9 and 1.1, and

with low LD with the existing 220 SNPs (r^2 < 0.1 and p-value > 0.05). However, only 25 of these SNPs were successfully genotyped, most likely because the primer sequences were not specific enough (results not shown). Third, we selected 149 SNPs from the control panel of Mosca *et al.* (2012) that had less than 5% missing data in that study. Of these, 129 SNPs were successfully genotyped. Both DNA isolation and genotyping was performed using KASP arrays and the all-inclusive service from LGC Genomics (Middlesex, UK).

Ten of the adult trees per population were measured for δ^{13}C. Needles were sampled in spring 2016 for 2015 grown needles. Approximately 80 mg freeze-dried needle material was milled in 2 ml polypropylene tubes equipped with a 5 mm glass ball at 30 Hz for 4 min. Subsamples of approximately 5 mg needle powder were combusted in an elemental analyzer (Flash EA by Thermo Finnigan,D- Bremen) coupled to an isotope ratio mass spectrometer (Delta XP by Thermo Finnigan,D- Bremen) by a Conflo II interface (Thermo Finnigan,D- Bremen).

Seedling common garden data

In April 2010, from three mother trees per population (subsequently called families) approximately 2000 seeds were sown in open-air nursery beds at the Swiss Federal Research Institute WSL in Birmensdorf, Switzerland (47°21′42″N, 8°27′22″E, 550 m a.s.l.). Families and populations were not replicated or randomized in the nursery because the soil was well mixed and the terrain was mostly flat, but the position of each seedling was recorded to check and control for spatial auto-correlation (see Supplementary Methods S1). In spring 2012, at least 12 randomly selected

viable seedlings per family were transplanted to an open experimental field site at Brunnersberg, a former pasture on a south facing slope (20-24% incline) in the Swiss Jura Mountains ($47°19'35''N$, $7°36'42''E$, 1090 m a.s.l.). Seedlings were planted at 30 $\times$ 40 cm spacing, provenances and families were randomized across 16 blocks. Both the nursery and common garden locations were within the natural range of silver fir. Note that the data presented here were part of a larger experiment involving more species and populations, see Frank *et al.* (2017b) for more details.

Phenotypic measurements used herein were performed during the fourth and fifth growing seasons, in 2013 and 2014 respectively. The 2013 measures were published in Frank *et al.* (2017b); see also Supplementary Methods S1. Traits included Terminal Bud Break (2013 and 2014, variable names capitalized hereafter) and Lateral Bud Break (2013) defined as the Julian date when the membrane below bud scales was broken and the first green needles became visible, Growth Cessation (2013) defined as the date when 95% of terminal leader height growth was achieved, Maximum Growth Rate (2013) calculated as the first derivative of the growth curve fitted to five to 17 height measures recorded during the growing season following the procedure proposed in Frank *et al.* (2017b), Growth Duration (2013) defined as time from Terminal Bud Break to Growth Cessation, Height (2013 and 2014) defined from the ground surface to the uppermost bud base, and Diameter (2013 and 2014) at 2 cm above ground surface. The latter two were measured after Growth Cessation. For clarity, we call Height and Diameter morphology traits, Maximum Growth Rate and Duration growth traits, and Terminal/Lateral Bud Break and Growth Cessation (equivalent to bud set) phenology traits. In total, we analyzed 880

observations. All traits were normally distributed, or could be approximated with a normal distribution in the case of discrete traits, and correlated with one another to a varying extent (Supporting Information Fig. S2).

Environmental data

We used downscaled historical climatic data to characterize environmental differences among populations. In order to obtain the closest representation of the climate of the period when the current populations were established, we used data from 1 January 1901 to 31 December 1978. The choice of this period was justified by two facts: (i) no observation-based climate data go back further in time, and (ii) starting from approximately 1980, the temperature time series are overwhelmed by the effect of global warming (Harris *et al.*, 2014). We used statistical downscaling using the delta method (Hay *et al.*, 2000) to obtain 1 km grid scale monthly minimum, maximum and mean temperature, and total precipitation fields for this period. The reference climatic data set was the 0.5° resolution CRU TS v. 4.01 data (20 September 2017 release, Harris *et al.* (2014)) available for the 1 January 1901 - 31 December 2016 period, while the downscaling was based on the overlapping period (i.e. 1 January 1979 - 31 December 2016) with the 1 km resolution CHELSA data (Karger *et al.*, 2017). Further, soil available water capacity (AWC) was obtained at a 250 m resolution from the Soilgrids data base (Hengl *et al.*, 2017).

We calculated the 19 bioclimatic variables (Booth *et al.*, 2014) using the R package dismo (Hijmans *et al.*, 2017), and two potential evapotranspiration (PET) indices and four standardized precipitation -

evapotranspiration index (SPEI) variables using the R package SPEI (Beguería & Vicente-Serrano, 2017), two indicators of late frost, and the self-calibrated Palmer's drought severity index or scPDSI (Wells *et al.* (2004), Table 1). SPEI and scPDSI were summarized as measures of drought severity and frequency across the full monthly time series (Table 1). All climatic variables were considered as raw values or as deviations from the common garden environment in Brunnersberg (based on the CHELSA data for the period of 1 January 1979 - 31 December 2013). However, the two ways of calculating the climate led to the same conclusions (results not shown), so we present results with the raw variables only for ease of interpretation.

Statistical analysis

We used the statistical framework developed by Ovaskainen *et al.* (2011) and Karhunen *et al.* (2014) with slight modifications. Briefly, this methodology integrates genetic, phenotypic and environmental data to test if trait differentiation measured in a common garden experiment reflects local adaptation, while accounting for past demography inferred from supposedly neutral molecular marker data, and to identify potential environmental drivers. The three steps of this analysis were (i) inference of the demography, (ii) estimation of the additive genetic trait values in a supposed ancestral population and contrasting these with their equivalents in the contemporary populations, and (iii) assessing if the deviations of additive genetic trait values from the ancestral values can be explained by environmental variation. We detail these steps in the following paragraphs (see also Supporting Information Fig. S1 for an overview).

First, we estimated the coancestry matrix (a.k.a. drift distances) between all pairs of populations from variation in SNP allele frequencies assuming an admixture F-model (AFM) and using a Metropolis-Hastings algorithm implemented in the R package *RAFM* (Karhunen & Ovaskainen, 2012). Further, we compared the posterior mean coancestry matrix against that estimated using the Bayesian clustering algorithm implemented in the software STRUCTURE v.2.3.4 (Falush *et al.*, 2003). See details of the demographic inference in Supplementary Methods S2.

Second, we used the method of Ovaskainen *et al.* (2011) to test if the estimated additive genetic trait values of the contemporary populations have diverged more from the ancestral value than expected by genetic drift only. We used a slightly modified version of the R package *driftsel* (Karhunen *et al.*, 2013) that co-estimates the ancestral variance-covariance matrix (G_A), the ancestral mean additive genetic trait values and the effect of covariates (i.e. the fixed effects), and the population effects (i.e. deviations from the ancestral mean) using a Bayesian mixed-effects animal model. This model is different from a classical animal model (reviewed in Kruuk *et al.* (2008)) in that it accounts simultaneously for the family structure of the common garden (i.e. the pedigree) and the drift distances (i.e. the demography) previously estimated from genetic marker data. In Ovaskainen *et al.* (2011) a single statistic, the S-statistic, is calculated to evaluate the overall evidence for selection across all populations. $S = 0.5$ indicates consistency with neutrality, $S = 0$ implies a match with purifying, and $S = 1$ with diversifying selection. In this study, we also assess to what extent the particular populations deviate from their neutral expectation (see Supplementary Methods S3 for details).

We tested all traits individually and all pairwise combinations between traits measured in the same year. Seed weight and block of the common garden were included as covariates. We ran three independent Markov chains of the Bayesian animal model using a burn-in of 50,000 iterations followed by 30,000 iterations for estimation for single traits, and a burn-in of 70,000 iterations followed by 30,000 iterations for estimation for trait pairs, both with a thinning interval of 20. The three independent chains converged to similar optima and led to the same conclusions concerning the signature of selection (potential scale reduction factor of the S-statistic ranged between 0.99 and 1.1 across all traits) for the single trait and two trait analysis. However, with more than two traits the convergence was no longer optimal, so we did not consider these higher order trait interactions.

Third, we attempted to identify the potential environmental drivers of adaptive divergence between populations. We used the H^*-test, which can be viewed as a standardized version of the H-test developed by Karhunen *et al.* (2014) (see Supplementary Methods S3 for more details). To avoid a multiple testing burden of 34 environmental variables in Table 1, we performed a Principal Component Analysis (PCA) on the standardized and scaled variables. The first five axes explained 84% of the variance, thus we performed a H^*-test for each of these PC axes only. The variables with the highest loadings on each of the PC axes were the following: PC1: bio.2 (Mean Diurnal Range) and Elevation, PC2: bio.10 (Mean Temperature of the Warmest Quarter) and PET.harg, PC3 and 4: none, PC5: bio.8 (Mean Temperature of the Warmest Quarter) and bio.15 (Precipitation seasonality). See Supporting Information Table S2 for the loadings of all environmental variables on the first five PC axes. The novel

methodological aspects detailed in Supplementary Methods S3, i.e. the procedure to evaluate adaptive divergence at each population, and the H^*-test are now implemented in the R package *driftsel*[1].

For a comparison with the Ovaskainen *et al.* (2011) approach, we also performed a classic $Q_{ST} - F_{ST}$ test using the bootstrap procedure described in Whitlock & Guillaume (2009) implemented in the R package QstFstComp (Gilbert & Whitlock, 2015)[2]. We considered a one-tailed test, because we were interested in testing for adaptive divergence only, thus Q_{ST} being significantly greater than F_{ST}.

Finally, the resemblance between the family members measured in the common garden experiment can also be exploited to estimate the evolutionary potential of the studied traits. Two commonly used measures of evolutionary potential are the heritability (h^2=V_A/V_P) and the additive genetic coefficient of variation (CV_A=σ_A/M) (Mittell *et al.*, 2015), where V_A is the additive genetic variance and σ_A is its square–root, V_P is the total phenotypic variance and M is the trait mean. CV_A is dimensionless, independent of other sources of variance, thus has been advocated for comparisons between traits (Houle, 1992, Hansen *et al.*, 2011).

Results

Population history

The STRUCTURE analysis and the estimated drift distances among populations using AFM indicated the presence of two main clusters that

[1] https://github.com/kcsillery/driftsel
[2] https://github.com/kjgilbert/QstFstComp

correspond to Eastern and Western Swiss populations (Fig. 1). In addition, the population POS did not belong to either of these two groups, which is plausible given its isolated geographic location on the south side of the Swiss Alps (Fig. 1). The posterior mean global F_{ST} across the 19 populations based on the coancestry matrix was 0.0184 (95% credible interval: 0.0167, 0.0202). In contrast, F_{ST} estimated with the Whitlock & Guillaume (2009) approach was 0.0056 (95% confidence interval: 0.0051, 0.0061). Both methods show that F_{ST} is small, which reflects recent divergence between Swiss populations (approximately 200 generations if we assume a colonization 8 kyr BP and a generation time of 40 years) and ongoing gene flow due to long-distance dispersal. Further, F_{ST} from *driftsel* is likely lower because *driftsel* explicitly models the demographic distances between populations, and it is less sensitive to the level of polymorphism in marker loci (Karhunen & Ovaskainen, 2012). Demographic distances between populations estimated using *RAFM* or the software STRUCTURE were similar; the highest similarity between the two was achieved for $K = 4$ in STRUCTURE (Mantel statistic of 0.891, which is similar to deviations between different chains of AFM; see Supplementary Methods S2 for more details).

Adaptive trait divergence across all populations

Similar degrees of adaptive divergence were revealed using the *S*-test of (Ovaskainen *et al.*, 2011) and classic $Q_{ST} - F_{ST}$ comparison (Whitlock & Guillaume, 2009) across traits (Table 2). Using either of the methods, the strongest signature of selection was observed for seedling Height followed by the Bud Break traits, then for Growth Duration and Diameter. Traits

measured both in 2013 and 2014 revealed similar signatures of selection, but in the $Q_{ST} - F_{ST}$ test Terminal Bud Break was only marginally significant in 2014. Maximum Growth Rate and Cessation showed no evidence of adaptive divergence in either of the tests due to their high within population variance (Table 2).

Several trait pairs showed a signature of selection using the *S*-test, mostly those that already did so in the single trait analysis (Fig. 2a). We extracted the genetic correlations between traits from the posterior mean ancestral *G*-matrix (G_A), and assessed if the 95% credible interval included zero (Fig. 2a, Supporting Information Table S3). Trait pairs that involved Height had the highest *S* statistics, but their genetic correlations did not differ from zero. Bud break often had high genetic correlations with growth traits and also high *S* values. The lowest *S* was observed between the Maximum Growth Rate and Growth Cessation (Fig. 2a). We used a standardized Mantel test following Cheverud (1988) to compare the phenotypic variance-covariance matrix (*P*-matrix) with G_A. The null hypothesis is no association between genetic and phenotypic matrices. The test was averaged across the posterior distribution of G_A. Five trait pairs had significantly different G_A- and *P*-matrices (Mantel-test, p>0.05), but only two had r_g different from zero (Supporting Information Table S3): Terminal and Lateral Bud Break, and Terminal Bud Break and Growth Duration. These two trait pairs were more strongly genetically correlated than expected based on the phenotypes (Fig. 2b). The posterior mean r_g was at its maximum value for Terminal and Lateral Bud Break, which is likely due to developmental constrains. Further, Terminal Bud Break and Growth Duration also had a 38% higher genetic than phenotypic

correlation (Fig. 2b).

Adaptive life-history strategies of particular populations

Unusual trait divergence at several populations contributed to the overall signature of selection using the *S* test. Fig. 3 shows, for each trait, how much each population diverged from the ancestral mean and if this divergence is more than expected by drift. The highest number of populations with adaptive divergence was observed for Height (Fig. 3a–b): seven (in 2013) and eight (in 2014) out of 19 populations deviated from their neutral expectations. All these outlier populations evolved towards a higher mean height and no populations have been selected for reduced height. The *S*-test revealed also a signature of selection for Diameter (Table 2), however, none of the particular populations showed unusual divergence (Fig. 3c–d). Yet, since there was a strong genetic correlation between Height and Diameter, the same populations showed the largest Diameter as for Height (Fig. 3a–d). The signature of selection on bud break traits was dominated by divergence in one population (SIR) that had unusually early bud break (Fig. 3e–g). Similarly, for Growth Duration, unusually longer growth duration was detected in two populations only, SIR and MGY (Fig. 3i).

In the two trait analysis, the correlated evolution of Bud Break and Growth Duration and Rate of particular populations became even more apparent (Fig. 4). SIR and MGY still showed a signature of selection, but at the opposite end of the trait space, and population VRG evolved towards late Terminal Bud Break and shorter Growth Duration. These patterns can be interpreted as contrasting life-history strategies. SIR and MGY followed

a "start early and grow slowly" strategy, i.e. they burst buds early and then grow for a long time at a low rate, while at the other end of trait space, population VRG followed a "start late and grow fast" strategy, i.e. bursts buds late, but then grows fast for a short period of time (Fig. 4).

Phenology and growth traits' posterior mean additive genetic trait values were significantly correlated with δ^{13}C in adult trees measured *in-situ* (2013 Terminal Bud Break, r=-0.54, p-value = 0.033; 2014 Terminal Bud Break r=-0.5, p-value = 0.055; 2013 Lateral Bud Break r=-0.56, p-value = 0.025, 2013 Maximum Growth Rate r=-0.53, p-value = 0.041; 2013 Growth Duration r=0.53, p-value = 0.037). The correlations with the phenology–growth complex were such that the "start early and grow slowly" seedling strategy had, on average, higher water use efficiency in adults, while the "start late and grow fast" seedling strategy low water use efficiency in adult trees (Fig. 4). In contrast, the other traits were not correlated with mean δ^{13}C (absolute value of r < 0.25 and p-value > 0.58). p-values were corrected for multiple testing using the method of correction for non-independent tests (Cheverud, 2001); see all additive trait value–mean δ^{13}C correlations in Supplementary Information Fig. S3.

Environmental drivers

Environmental PC axes explained a non-zero proportion of the trait divergence for most traits, but the highest correlations (>90%) were obtained for Height, Lateral Bud Break and Growth Duration (Table 3). Notice that, not surprisingly, these traits showed a signature of selection with the *S*-tests (Table 2 and Fig. 3). For each of these traits a particular aspect of the environment mattered. For Height, and also for Diameter to

some extent, environmental PC axis 1 showed the highest correlations with trait divergence (Table 3). The raw environmental variables that had the highest loadings on PC1 were variables related to the mean and variance in temperature, such as Annual Mean Temperature (bio.1), Elevation, potential evapotranspiration (PET.thorn), Late frost (late.frost2), or Isothermality (bio.3) (see the list of top ten variables in Table S2). Fig. 5a shows the full environmental space defined by PC1 and PC4, which was the second most important axis for Height: populations that evolved towards a taller stature are situated in the warmer and more thermally stable part of the climatic space.

For the phenology–growth complex, PC axes 2 and 5 had the highest correlations with trait divergence (Table 3). The environmental variables with the highest loadings on these axes were principally variables related to the mean and variance in precipitation, such as Annual Precipitation (bio.12), Precipitation Seasonality (bio.15), Precipitation of Wettest Quarter (bio.16) (see the list of top ten variables in Table S2). Thus, the "start early and grow slowly" seedling strategy of SIR and MGY, together with their high water use efficiency as adult trees (Fig. 4), has potentially evolved as a response to the low yearly total amount of precipitation (755mm in SIR and 801mm in MGY) and low precipitation seasonality (Fig. 5b). At the other end of the trait space, the climate of population VRG is characterized by high levels of yearly total precipitation (1621mm) and ample winter snow as reflected by its higher precipitation seasonality (Fig. 5b).

Evolutionary potential

We found the highest potential for evolution in three growth traits: Maximum Growth Rate, Growth Duration and Diameter, while spring phenology showed the lowest potential for evolution (Table 2). Estimating the additive genetic variance across the 19 populations and 57 families (three families per population) involves the assumption that the additive genetic variance is constant across the sampling area. We tested this hypothesis using the larger data set used by Frank *et al.* (2017b) involving 4107 observations from 91 populations and 259 families. We found that estimates of CV_A were not strongly affected by the reduction in sample size, and h^2 and CV_A were similar across three main geographic regions of Switzerland (Supplementary Methods S1), suggesting that our sample size was sufficient to estimate the evolutionary potential across the 19 populations.

Discussion

Are there general patterns of adaptation across a heterogeneous environment?

In this study, we found evidence for locally adapted life-history strategies across a heterogeneous Alpine landscape. The high number of populations leveraged the power of classical $Q_{ST} - F_{ST}$ tests and led to similar global conclusions than the *S*-test of Ovaskainen *et al.* (2011) (Table 2). However, using our novel methodology, we were also able to identify adaptive

life-history strategies in a multi-trait space and pinpoint which populations show a signature of adaptive divergence (Ovaskainen *et al.* (2011) and Supplementary Methods S3). In particular, we identified two groups of correlated characters whose evolution could be driven by the environmental cues. First, our results suggest that the two morphological characters, Height and Diameter, evolve in a correlated manner, and that warmer and more thermally stable environments select for larger stature (Fig. 5a). Second, we identified a phenology–growth trait complex that may evolve in response to precipitation. Populations from areas characterized by generally low levels of precipitation (i.e. with drought) evolved to start the growing season early and then grow slowly, and also to have a high water use efficiency (Fig. 4 and 5b). These populations, SIR and MGY, originate from a dry inner Alpine valley of Switzerland, the Rhône Valley. Further, the other Rhône Valley populations, GRY and BRS, and populations from other areas of Switzerland with a similar climate, such as the Rhine valley (JEZ) and Ticino (PRA) are also the closest in the phenology–growth trait space to SIR and MGY (Fig. 1). In contrast, VRG, situated in a valley characterized by ample precipitation, evolved towards a "start late and grow fast" strategy. Again, independent data from adult trees corroborated our findings, VRG, and other populations from humid sites, such as GRB and MUO, had a low water use efficiency (Fig. 4).

The length of the annual development cycle of temperate trees is constrained between two opposing forces: maximizing the length of the vegetative season while avoiding late frost and summer drought. This life-history trade-off is particularly important in mountainous environments, where the length of the growing season is often limited by

late snow or compromised by summer drought in dry, inner Alpine valleys. Our study region is relatively small, and limited to one part of the Alpine Range. However, the correlation between the phenology–growth life-history trade-off in seedlings and water use efficiency in adults provides independent evidence for this trade-off (Fig. 4), and supports the existence of a general pattern of adaptation across a mountainous landscape. Thus, we speculate that the phenology–growth life-history trade-off may be more general across other mountainous regions and provide a testable prediction in other mountain ranges and species.

Why are some traits under selection and not others?

Demonstrating selection for taller stature in a tree is not surprising because tall stature has numerous fitness advantages. Taller seedlings/young trees have access to more light and can out-compete their neighbors, and high stature in mature trees can facilitate pollen and seed dispersal (Petit & Hampe, 2006). Interestingly, at least some of the populations that appear to have been selected for larger stature (Fig. 3a–b) are located on the Swiss Plateau, where the effect of forest management cannot be fully excluded (*e.g.* Bürgi & Schuler, 2003). Since tree height is also a key trait from an economical point of view, there is a possibility that the observed patterns are, in part, a result of artificial selection for height.

A long-standing hypothesis in evolutionary biology is that traits belonging to the same functional and/or developmental group are genetically more integrated than traits with different functions or developmental origins (Berg, 1960, Pigliucci & Preston, 2004). Several empirical studies found evidence that there is greater genetic and

phenotypic character integration within suites of functionally or developmentally related traits than between them, *e.g.* within or between floral vs. vegetative traits in plants (Waitt & Levin, 1998, Baranzelli *et al.*, 2014). Here, we found two trait pairs with an ancestral *G*-matrix that was significantly different from the *P*-matrix, and in both cases the genetic correlation was significantly higher than the phenotypic correlation. First, between Terminal and Lateral Bud Break the genetic correlation was one, which illustrates a complete character integration (Fig. 2b). Second, between Terminal Bud Break and Growth Duration (Fig. 4), which suggests that at the physiological and molecular level, spring phenology and growth are strongly linked.

There is overwhelming evidence of adaptive clines for bud set (a proxy for growth cessation) in many forest tree species, including conifers, but none in *Abies* species (Alberto *et al.*, 2013). Consistently, in this study, Growth Cessation did not show evidence of adaptive divergence. The explanation may lie in the deterministic bud development of *Abies* species (Cooke *et al.*, 2012). They produce terminal buds during the summer at the tip of each leading branch shoot and remain dormant during the following winter. Each bud contains a preformed stem unit composed of internodes and leaf primordia that will grow to branches and photosynthesizing needles, respectively, during the following growing season.

Potential limitations and caveats

Adaptive trait divergence may be a result of local adaptation or adaptive phenotypic plasticity (Merilä & Hendry, 2014). To tell these two apart, one has to measure trait values of a particular genotype across different

environments. Common garden studies of forest trees often observe site-specific effects for growth or phenology, indicative of adaptive plasticity (Alberto *et al.*, 2013). For example, Santos-del Blanco *et al.* (2013) found a growth-reproduction trade-off in *Pinus halepensis*, with trees in high stress sites investing more in reproduction and trees in low stress sites investing more in vegetative growth. Here, we only had a single common garden and the relocation to Jura did not affect all provenances the same way. Thus, we could not distinguish between local adaptation and adaptive plasticity. Nevertheless, even if plasticity is known to play an important role in explaining phenotypic differences, the signature of adaptive divergence is often confirmed across all tested common garden sites (*e.g.* Rodríguez-Quilón *et al.*, 2016).

Plasticity could have also caused the observed spatial variation in δ^{13}C measured in adult trees *in-situ*. It appears that the importance of plastic and genetic factors is species specific even among conifers. For example, in *Pinus sylvestris*, Santini *et al.* (2018) suggested that plastic, and not genetic, responses dominate the inter-population variability in water use efficiency, even though, admittedly they did not have progeny information. In contrast, Voltas *et al.* (2008) reported large genetic differences among populations in *Pinus halepensis* using a common garden trial. δ^{13}C is also prone to temporal, year-to-year, fluctuations because it integrates the photosynthetic activity through the period the tissue was synthesized, which is a single growing season. While measures of δ^{13}C are often correlated across years (*e.g.* Chevillat *et al.*, 2005), environment can also have an effect (*e.g.* Rinne *et al.*, 2015). For example, a temporal increase in water use efficiency due to anthropogenic CO_2 and N fertilization have

been reported across different forest tree species across Europe (Saurer *et al.*, 2014). Finally, spatial variation, notably latitudinal and altitudinal trends, in δ^{13}C have long been demonstrated (Körner *et al.*, 1991). However, it is often difficult to pinpoint single environmental variables across regional or continental spatial scales that explain the variation in δ^{13}C (Leonardi *et al.*, 2012). Thus, we estimated that any attempts for environmental corrections of the population mean δ^{13}C would lack a solid basis.

Common garden studies that use seeds from wild populations may provide inaccurate estimates of population differentiation, particularly for early traits, due to environmental maternal effects (Bossdorf *et al.*, 2005). Quantitative genetic studies that control for genetic and/or epigenetic maternal effects in forest trees are still rare (Alberto *et al.*, 2013). Although there is evidence for long-lasting effects of seed size in *Pines* (Zas & Sampedro, 2015, Surles *et al.*, 1993), such effects are less obvious in other conifers (St. Clair & Adams, 1991). Nevertheless, we controlled for the average seed weight of the families in the Bayesian animal model (see also Supplementary Methods S1), which is admittedly just one component of the maternal effects. More recently, the role of epigenetic "memory" effects has been demonstrated in forest trees (Prunier *et al.*, 2016). For example, a common garden transplantation experiment of Norway spruce and European larch found that the previous year's environment and provenance contributed to the current year's bud break phenology (Gömöry *et al.*, 2015). Similar effects could have played a role in our experiments, however, all populations experienced the same year-to-year environmental fluctuations.

The design of the common garden study suffers from three potential limitations. First, for height, the results might be sensitive to non-randomization in the nursery (see Supplementary Methods S1). Seedlings were likely stressed from the replanting from the nursery to the common garden location in 2012, which may still be detectable in 2013 Height (Supplementary Methods S1), and in 2014, a frost event in March damaged some seedlings. However, even with this new stress, the evidence for adaptive trait differentiation was almost identical to that in 2013 (*e.g.* Fig. 3). Second, we had phenotypic observations from three families per population, which is rather low. Nevertheless, using the full phenotypic data set of Frank *et al.* (2017b) across 91 populations, we were able to combine populations from nearby regions, thereby increasing the number of families to 5.3 families per population, on average. We found that estimates of evolutionary potential and also Q_{ST} were extremely similar to those obtained from three families (Supplementary Methods S1). Third, we estimated the evolutionary potential, in particular, the evolvability, across many populations, thereby assuming that the additive genetic variance is constant across the study region. Laboratory experiments have shown that the *G*-matrix can change in response to drift or selection, but maybe not in the wild (Delahaie *et al.*, 2017). To test this hypothesis, we estimated the h^2 and CV_A separately for the three main climatic regions as defined by foresters. We found that the evolutionary potential was similar across the three regions (Supplementary Methods S1), suggesting that the assumption of constant additive genetic variance across Swiss populations is acceptable. Overall we found that CV_A was much more robust to any of the three above-cited issues than h^2, in agreement with previous studies

(Houle, 1992, Hansen *et al.*, 2011).

Practical implications and the future of silver fir in the study area

Silver fir has been identified as a conifer with great ecological and economic potential for the future because of its high tolerance to bark beetle attacks (Wermelinger, 2004), and because it may cope well with drought stress (Lebourgeois *et al.*, 2013, Vitali *et al.*, 2017, Frank *et al.*, 2017a). Nevertheless, silver fir may already be threatened in some Mediterranean areas, where die-back events have been documented (Cailleret *et al.*, 2014), or in Southwestern Europe, where reduced growth has been reported (Gazol *et al.*, 2015). In this study we found that silver fir was able to evolve to a taller stature in warm and thermally stable regions, such as the Swiss Plateau. Indeed, positive effects of climate warming have been observed in temperate forest trees, where warming enhanced growth (Gazol *et al.*, 2015). Since height, diameter and growth rate have the highest evolvability and strongest signature of selection among the studied traits (Table 2), we may speculate that some populations will respond with enhanced growth. However, the predicted pace of climate change is much faster than it has been during post-glacial expansion/re-colonization, thus assisted migration may provide a practical solution to overcome this rapid rate of change (Aitken & Bemmels, 2016). Based on our results, populations of the Rhône and Rhine Valleys could provide drought tolerant seed sources for future plantations in other parts of Switzerland.

Data archiving

SNP and δ^{13}C data have been submitted to Dryad (`https://doi.org/10.5061/dryad.s205vd8`).

Acknowledgements:

We thank all members of the ADAPT project that provided the phenotypic data for this study, especially Aline Frank, Caroline Heiri and Peter Brang, and to the leader of the EADAPT project, Andrea Kupferschmid, who provided the height and diameter data for 2014. The project was funded by a research grant from the Center for Adaptation to a Changing Environment (ACE) at the ETH Zurich. KC was supported by an ACE fellowship and by a Marie Skłodowska-Curie fellowship (FORGENET). We thank Kristian Ullrich for help with the SNP selection, and Dirk Karger with extracting the climatic data from the data bases. The contribution of several field and lab workers was necessary for the sample collection and preparation for DNA extraction and genotyping, in particular, we thank Catherine Folly, René Graf, and Olivier Charlandie. We thank Annika Ackermann (Grassland Isolab, ETH Zurich), who performed the stable isotope measures, and Fabian Deuber for sample preparation.

Compliance with ethical standards

Conflict of interest

The authors declare that they have no conflict ofinterest.

References

Ackerly D, Loarie S, Cornwell W, Weiss S, Hamilton H, Branciforte R, Kraft N (2010) The geography of climate change: implications for conservation biogeography. *Divers Distrib*, **16**: 476–487.

Aitken SN, Bemmels JB (2016) Time to get moving: assisted gene flow of forest trees. *Evol Appl*, **9**: 271–290.

Alberto F, Bouffier L, Louvet JM, Lamy JB, Delzon S, Kremer A (2011) Adaptive responses for seed and leaf phenology in natural populations of sessile oak along an altitudinal gradient. *J Evol Biol*, **24**: 1442–1454.

Alberto FJ, Aitken SN, Alía R, *et al.* (2013) Potential for evolutionary responses to climate change - evidence from tree populations. *Global Change Biol*, **19**: 1645–1661.

Austin MP, Van Niel KP (2011) Improving species distribution models for climate change studies: variable selection and scale. *J Biogeogr*, **38**: 1–8.

Baranzelli MC, Sérsic AN, Cocucci AA (2014) The search for Pleiades in trait constellations: Functional integration and phenotypic selection in the complex flowers of Morrenia brachystephana (Apocynaceae). *J Evol Biol*, **27**: 724–736.

Beguería S, Vicente-Serrano SM (2017) SPEI: calculation of the standardised precipitation-evapotranspiration index. *R package version 1.7*, **1**.

Berg R (1960) The ecological significance of correlation pleiades. *Evolution*, **14**: 171–180.

721 Booth TH, Nix HA, Busby JR, Hutchinson MF (2014) Bioclim: the first species
722 distribution modelling package, its early applications and relevance to
723 most current maxent studies. *Divers Distrib*, **20**: 1–9.

724 Bossdorf O, Auge H, Lafuma L, Rogers WE, Siemann E, Prati D (2005)
725 Phenotypic and genetic differentiation between native and introduced
726 plant populations. *Oecologia*, **144**: 1–11.

727 Brendel O, Le Thiec D, Scotti-Saintagne C, Bodénès C, Kremer A, Guehl JM
728 (2008) Quantitative trait loci controlling water use efficiency and related
729 traits in *Quercus robur* L. *Tree Genet Genomes*, **4**: 263–278.

730 Brendel O, Pot D, Plomion C, Rozenberg P, Guehl JM (2002) Genetic
731 parameters and QTL analysis of δ^{13}c and ring width in maritime pine.
732 *Plant Cell Environ*, **25**: 945–953.

733 Burga CA, Hussendörfer E (2001) Vegetation history of *Abies alba* Mill. (silver
734 fir) in Switzerland–pollen analytical and genetic surveys related to aspects
735 of vegetation history of *Picea abies* (L.) H. Karsten (Norway spruce). *Veg*
736 *Hist Archaeobot*, **10**: 151–159.

737 Bürgi M, Schuler A (2003) Driving forces of forest management - an analysis
738 of regeneration practices in the forests of the Swiss Central Plateau during
739 the 19th and 20th century. *For Ecol Manage*, **176**: 173–183.

740 Cailleret M, Nourtier M, Amm A, Durand-Gillmann M, Davi H (2014)
741 Drought-induced decline and mortality of silver fir differ among three sites
742 in Southern France. *Ann For Sci*, **71**: 1–15.

743 Chenoweth SF, Blows MW (2008) Q_{ST} meets the G matrix: The

744 dimensionality of adaptive divergence in multiple correlated quantitative
745 traits. *Evolution*, **62**: 1437–1449.

746 Cheverud JM (1988) A comparison of genetic and phenotypic correlations.
747 *Evolution*, **42**: 958–968.

748 Cheverud JM (2001) A simple correction for multiple comparisons in interval
749 mapping genome scans. *Heredity*, **87**: 52–58.

750 Chevillat VS, Siegwolf RT, Pepin S, Körner C (2005) Tissue-specific variation
751 of δ^{13}c in mature canopy trees in a temperate forest in central Europe.
752 *Basic Appl Ecol*, **6**: 519–534.

753 Chevin LM, Lande R (2010) When do adaptive plasticity and genetic
754 evolution prevent extinction of a density-regulated population? *Evolution*,
755 **64**: 1143–1150.

756 Cooke JE, Eriksson ME, Junttila O (2012) The dynamic nature of bud
757 dormancy in trees: environmental control and molecular mechanisms.
758 *Plant Cell Environ*, **35**: 1707–1728.

759 Dawson TE, Mambelli S, Plamboeck AH, Templer PH, Tu KP (2002) Stable
760 isotopes in plant ecology. *Annu Rev Ecol Syst*, **33**: 507–559.

761 De Kort H, Vander Mijnsbrugge K, Vandepitte K, Mergeay J, Ovaskainen O,
762 Honnay O (2016) Evolution, plasticity and evolving plasticity of phenology
763 in the tree species *Alnus glutinosa*. *J Evol Biol*, **29**: 253–264.

764 Delahaie B, Charmantier A, Chantepie S, Garant D, Porlier M, Teplitsky
765 C (2017) Conserved g-matrices of morphological and life-history traits
766 among continental and island blue tit populations. *Heredity*, **119**: 76.

767 Falush D, Stephens M, Pritchard JK (2003) Inference of population structure
768 using multilocus genotype data: linked loci and correlated allele
769 frequencies. *Genetics*, **164**: 1567–1587.

770 Farquhar GD, Ehleringer JR, Hubick KT (1989) Carbon isotope discrimination
771 and photosynthesis. *Annu Rev Plant Biol*, **40**: 503–537.

772 Frank A, Howe GT, Sperisen C, Brang P, Clair JBS, Schmatz DR, Heiri C
773 (2017a) Risk of genetic maladaptation due to climate change in three major
774 European tree species. *Global Change Biol*, **23**: 5358–5371.

775 Frank A, Sperisen C, Howe GT, Brang P, Walthert L, Clair JBS, Heiri C (2017b)
776 Distinct genecological patterns in seedlings of Norway spruce and silver
777 fir from a mountainous landscape. *Ecology*, **98**: 211–227.

778 Gaspar MJ, Louzada JL, Silva ME, Aguiar A, Almeida MH (2008) Age trends in
779 genetic parameters of wood density components in 46 half-sibling families
780 of *Pinus pinaster*. *Can J For Res*, **38**: 1470–1477.

781 Gazol A, Camarero JJ, Gutiérrez E, *et al.* (2015) Distinct effects of climate
782 warming on populations of silver fir (*Abies alba*) across Europe. *J Biogeogr*,
783 **42**: 1150–1162.

784 Gilbert KJ, Whitlock MC (2015) $Q_{ST} - F_{ST}$ comparisons with unbalanced
785 half-sib designs. *Mol Ecol Resour*, **15**: 262–267.

786 Gömöry D, Foffová E, Longauer R, Krajmerová D (2015) Memory effects
787 associated with early-growth environment in Norway spruce and
788 European larch. *Eur J Forest Res*, **134**: 89–97.

Hampe A, Petit RJ (2005) Conserving biodiversity under climate change: the rear edge matters. *Ecol Lett*, **8**: 461–467.

Hansen TF, Pélabon C, Houle D (2011) Heritability is not evolvability. *Evol Biol*, **38**: 258.

Harris I, Jones P, Osborn T, Lister D (2014) Updated high-resolution grids of monthly climatic observations–the CRU TS3.10 Dataset. *Int J Climatol*, **34**: 623–642.

Hay LE, Wilby RL, Leavesley GH (2000) A comparison of delta change and downscaled GCM scenarios for three mountainous basins in the United States. *J Am Water Resour Assoc*, **36**: 387–397.

Hengl T, de Jesus JM, Heuvelink GB, *et al.* (2017) SoilGrids250m: Global gridded soil information based on machine learning. *PLoS One*, **12**: e0169748.

Hewitt GM (1999) Post-glacial re-colonization of european biota. *Biol J Linn Soc*, **68**: 87–112.

Hijmans RJ, Phillips S, Leathwick J, Elith J, Hijmans MRJ (2017) Package 'dismo'. *Circles*, **9**.

Houle D (1992) Comparing evolvability and variability of quantitative traits. *Genetics*, **130**: 195–204.

Johnsen KH, Flanagan LB, Huber DA, Major JE (1999) Genetic variation in growth, carbon isotope discrimination, and foliar N concentration in *Picea mariana*: analyses from a half-diallel mating design using field-grown trees. *Can J For Res*, **29**: 1727–1735.

Karger DN, Conrad O, Böhner J, *et al.* (2017) Climatologies at high resolution for the Earth's land surface areas. *Sci Data*, **4**: 170122.

Karhunen M, Merilä J, Leinonen T, Cano JM, Ovaskainen O (2013) driftsel: An R package for detecting signals of natural selection in quantitative traits. *Mol Ecol Resour*, **13**: 746–754.

Karhunen M, Ovaskainen O (2012) Estimating population-level coancestry coefficients by an admixture F model. *Genetics*, **192**: 609–617.

Karhunen M, Ovaskainen O, Herczeg G, Merilä J (2014) Bringing habitat information into statistical tests of local adaptation in quantitative traits: A case study of nine-spined sticklebacks. *Evolution*, **68**: 559–568.

Kawecki TJ (2008) Adaptation to marginal habitats. *Annu Rev Ecol Evol Syst*, **39**: 321–342.

Kawecki TJ, Ebert D (2004) Conceptual issues in local adaptation. *Ecol Lett*, **7**: 1225–1241.

Körner C, Farquhar G, Wong S (1991) Carbon isotope discrimination by plants follows latitudinal and altitudinal trends. *Oecologia*, **88**: 30–40.

Kremer A, Ronce O, Robledo-Arnuncio JJ, *et al.* (2012) Long-distance gene flow and adaptation of forest trees to rapid climate change. *Ecol Lett*, **15**: 378–392.

Kruuk LE, Slate J, Wilson AJ (2008) New Answers for Old Questions: The Evolutionary Quantitative Genetics of Wild Animal Populations. *Annu Rev Ecol Evol Syst*, **39**: 525–548.

834 Kunstler G, Albert CH, Courbaud B, *et al.* (2011) Effects of competition on
835 tree radial-growth vary in importance but not in intensity along climatic
836 gradients. *J Ecol*, **99**: 300–312.

837 Lebourgeois F, Gomez N, Pinto P, Mérian P (2013) Mixed stands reduce *Abies*
838 *alba* tree-ring sensitivity to summer drought in the Vosges mountains,
839 Western Europe. *For Ecol Manage*, **303**: 61–71.

840 Leonardi S, Gentilesca T, Guerrieri R, *et al.* (2012) Assessing the effects of
841 nitrogen deposition and climate on carbon isotope discrimination and
842 intrinsic water-use efficiency of angiosperm and conifer trees under rising
843 CO_2 conditions. *Global Change Biol*, **18**: 2925–2944.

844 Liepelt S, Bialozyt R, Ziegenhagen B (2002) Wind-dispersed pollen mediates
845 postglacial gene flow among refugia. *Proc Natl Acad Sci U S A*, **99**: 14590–
846 14594.

847 Liepelt S, Cheddadi R, de Beaulieu JL, *et al.* (2009) Postglacial range
848 expansion and its genetic imprints in *Abies alba* (Mill.) - A synthesis from
849 palaeobotanic and genetic data. *Rev Palaeobot Palynol*, **153**: 139–149.

850 Lind BM, Menon M, Bolte CE, Faske TM, Eckert AJ (2018) The genomics
851 of local adaptation in trees: Are we out of the woods yet? *Tree Genet*
852 *Genomes*, **14**: 29.

853 Martin G, Chapuis E, Goudet J (2008) Multivariate Q_{ST}–F_{ST} comparisons: A
854 neutrality test for the evolution of the G matrix in structured populations.
855 *Genetics*, **180**: 2135–2149.

856 McDowell NG, Ryan MG, Zeppel MJ, Tissue DT (2013) Feature: Improving

857 our knowledge of drought-induced forest mortality through experiments,
858 observations, and modeling. *New Phytol*, **200**: 289–293.

859 Merilä J, Hendry AP (2014) Climate change, adaptation, and phenotypic
860 plasticity: the problem and the evidence. *Evol Appl*, **7**: 1–14.

861 Mittell EA, Nakagawa S, Hadfield JD (2015) Are molecular markers useful
862 predictors of adaptive potential? *Ecol Lett*, **18**: 772–778.

863 Moran E, Lauder J, Musser C, Stathos A, Shu M (2017) The genetics of drought
864 tolerance in conifers. *New Phytol*, **216**: 1034–1048.

865 Mosca E, Eckert AJ, Di Pierro EA, Rocchini D, La Porta N, Belletti P, Neale
866 DB (2012) The geographical and environmental determinants of genetic
867 diversity for four alpine conifers of the European Alps. *Mol Ecol*, **21**: 5530–
868 5545.

869 Neale DB, Kremer A (2011) Forest tree genomics: growing resources and
870 applications. *Nat Rev Genet*, **12**: 111–122.

871 Ovaskainen O, Karhunen M, Zheng C, Arias JMC, Merilä J (2011) A new
872 method to uncover signatures of divergent and stabilizing selection in
873 quantitative traits. *Genetics*, **189**: 621–632.

874 Petit RJ, Hampe A (2006) Some evolutionary consequences of being a tree.
875 *Annu Rev Ecol Evol Syst*, **37**: 187–214.

876 Pigliucci M, Preston KA (2004) *Phenotypic integration: studying the ecology
877 and evolution of complex phenotypes*. Oxford University Press, Oxford, UK.

878 Polechova J (2018) Is the sky the limit? on the expansion threshold of a
879 species' range. *PLoS Biol*, **16**: e2005372.

Prunier J, Verta JP, MacKay JJ (2016) Conifer genomics and adaptation: at the crossroads of genetic diversity and genome function. *New Phytol*, **209**: 44–62.

Rehfeldt GE, Tchebakova NM, Parfenova YI, Wykoff WR, Kuzmina NA, Milyutin LI (2002) Intraspecific responses to climate in *Pinus sylvestris*. *Global Change Biol*, **8**: 912–929.

Resende M, Munoz P, Acosta J, *et al.* (2012) Accelerating the domestication of trees using genomic selection: accuracy of prediction models across ages and environments. *New Phytol*, **193**: 617–624.

Rinne KT, Saurer M, Kirdyanov AV, Bryukhanova MV, Prokushkin AS, Churakova O, Siegwolf RT (2015) Examining the response of needle carbohydrates from Siberian larch trees to climate using compound-specific δ^{13}C and concentration analyses. *Plant Cell Environ*, **38**: 2340–2352.

Rodríguez-Quilón I, Santos-del Blanco L, Serra-Varela MJ, Koskela J, González-Martínez SC, Alía R (2016) Capturing neutral and adaptive genetic diversity for conservation in a highly structured tree species. *Ecol Appl*, **26**: 2254–2266.

Roschanski AM, Csilléry K, Liepelt S, *et al.* (2016) Evidence of divergent selection for drought and cold tolerance at landscape and local scales in *Abies alba* Mill. in the French Mediterranean Alps. *Mol Ecol*, **25**: 776–794.

Ruosch M, Spahni R, Joos F, Henne PD, van der Knaap WO, Tinner W (2016) Past and future evolution of *Abies alba* forests in Europe - comparison of

903 a dynamic vegetation model with palaeo data and observations. *Global*
904 *Change Biol*, **22**: 727–740.

905 Santini F, Ferrio J, Hereş AM, *et al.* (2018) Scarce population genetic
906 differentiation but substantial spatiotemporal phenotypic variation of
907 water-use efficiency in *Pinus sylvestris* at its western distribution range.
908 *Eur Journal For Res*, **137**: 863–878.

909 Santos-del Blanco L, Bonser S, Valladares F, Chambel M, Climent J (2013)
910 Plasticity in reproduction and growth among 52 range-wide populations
911 of a Mediterranean conifer: adaptive responses to environmental stress. *J*
912 *Evol Biol*, **26**: 1912–1924.

913 Saurer M, Spahni R, Frank DC, *et al.* (2014) Spatial variability and temporal
914 trends in water-use efficiency of european forests. *Global Change Biol*, **20**:
915 3700–3712.

916 Savolainen O, Pyhäjärvi T, Knürr T (2007) Gene flow and local adaptation in
917 trees. *Annu Rev Ecol Evol Syst*, **38**: 595–619.

918 Schäfer MA, Berger D, Rohner PT, *et al.* (2018) Geographic clines in wing
919 morphology relate to colonization history in New World but not Old
920 World populations of yellow dung flies. *Evolution*, **72**: 1629–1644.

921 St Clair J, Adams W (1991) Effects of seed weight and rate of emergence on
922 early growth of open-pollinated Douglas-fir families. *For Sci*, **37**: 987–997.

923 Sultan SE, Spencer HG (2002) Metapopulation structure favors plasticity over
924 local adaptation. *Am Nat*, **160**: 271–283.

925 Surles SE, White TL, Hodge GR, Duryea ML (1993) Relationships among seed
926 weight components, seedling growth traits, and predicted field breeding
927 values in slash pine. *Can J For Res*, **23**: 1550–1556.

928 Van der Knaap W, van Leeuwen JF, Finsinger W, *et al.* (2005) Migration and
929 population expansion of *Abies*, *Fagus*, *Picea*, and *Quercus* since 15000 years
930 in and across the Alps, based on pollen-percentage threshold values. *Quat*
931 *Sci Rev*, **24**: 645–680.

932 Via S, Lande R (1985) Genotype-environment interaction and the evolution
933 of phenotypic plasticity. *Evolution*, **39**: 505–522.

934 Vitali V, Büntgen U, Bauhus J (2017) Silver fir and Douglas fir are more
935 tolerant to extreme droughts than Norway spruce in south-western
936 Germany. *Global Change Biol*, pp. 5108–5119.

937 Vitasse Y, Bresson CC, Kremer A, Michalet R, Delzon S (2010) Quantifying
938 phenological plasticity to temperature in two temperate tree species. *Funct*
939 *Ecol*, **24**: 1211–1218.

940 Voltas J, Chambel MR, Prada MA, Ferrio JP (2008) Climate-related variability
941 in carbon and oxygen stable isotopes among populations of aleppo pine
942 grown in common-garden tests. *Trees*, **22**: 759–769.

943 Waitt DE, Levin DA (1998) Genetic and phenotypic correlations in plants: a
944 botanical test of Cheverud's conjecture. *Heredity*, **80**: 310–319.

945 Wells N, Goddard S, Hayes MJ (2004) A self-calibrating Palmer drought
946 severity index. *J Climate*, **17**: 2335–2351.

947 Wermelinger B (2004) Ecology and management of the spruce bark beetle *Ips*
948 *typographus*–a review of recent research. *For Ecol Manage*, **202**: 67–82.

949 Whitlock MC (2008) Evolutionary inference from Q_{ST}. *Mol Ecol*, **17**: 1885–
950 1896.

951 Whitlock MC, Guillaume F (2009) Testing for spatially divergent selection:
952 comparing Q_{ST} to F_{ST}. *Genetics*, **183**: 1055–1063.

953 Yeaman S, Jarvis A (2006) Regional heterogeneity and gene flow maintain
954 variance in a quantitative trait within populations of lodgepole pine. *Proc*
955 *R Soc London, Ser B*, **273**: 1587–1593.

956 Zas R, Sampedro L (2015) Heritability of seed weight in maritime pine,
957 a relevant trait in the transmission of environmental maternal effects.
958 *Heredity*, **114**: 116.

Table 1: Geography and environmental variables calculated for the period of 1 January 1901 - 31 December 1978 from monthly mean, minimum and maximum temperature and total precipitation (CRU TS v. 4.01 data Harris *et al.* (2014) downscaled using CHELSA (Karger *et al.*, 2017)), and available water capacity (AWC, Soilgrids data base Hengl *et al.* (2017)). Abbreviations: PET: Potential Evapotranspitation; scPDSI: Palmer's Drought Severity Index, SPEI: Standardised Precipitation-Evapotranspiration Index.

Variable	Description	Mean	(Min., Max.)
Geography			
Long	Longitude (degrees)	8.3	(6.2, 10.5)
Lat	Latitude (degrees)	46.7	(46.1, 47.3)
Elev	Elevation (m a.s.l)	1062.2	(481, 1602.5)
Slope	Slope (%)	40	(0, 70)
Standard bioclimatic indexes			
bio.1	Annual Mean Temperature	6.1	(3.1, 9.3)
bio.2	Mean Diurnal Range (Mean of monthly Tmax - Tmin))	8.9	(8.6, 9.2)
bio.3	Isothermality (bio.2/bio.7) (* 100)	23.9	(23.2, 24.6)
bio.4	Temperature Seasonality (standard deviation *100)	663.7	(636.4, 676.9)
bio.5	Max Temperature of Warmest Month	24.2	(21, 27.4)
bio.6	Min Temperature of Coldest Month	-13	$(-15.8, -10)$
bio.7	Temperature Annual Range (bio.5-bio.6)	37.2	(36.2, 37.9)
bio.8	Mean Temperature of Wettest Quarter	9.5	$(-2.6, 17.7)$
bio.9	Mean Temperature of Driest Quarter	-1.7	$(-6.1, 3.9)$
bio.10	Mean Temperature of Warmest Quarter	16.8	(13.8, 20)
bio.11	Mean Temperature of Coldest Quarter	-6	$(-8.5, -3.3)$
bio.12	Annual Precipitation	1176.4	(505.6, 1690.9)
bio.13	Precipitation of Wettest Month	281	(128.1, 432.6)
bio.14	Precipitation of Driest Month	4	(0.4, 9.1)
bio.15	Precipitation Seasonality (Coefficient of Variation)	50	(46, 55.3)
bio.16	Precipitation of Wettest Quarter	641.2	(274.2, 1024.7)
bio.17	Precipitation of Driest Quarter	55.6	(24.5, 83.7)
bio.18	Precipitation of Warmest Quarter	277.3	(156, 442.9)
bio.19	Precipitation of Coldest Quarter	222.7	(65.6, 452.7)
Drought			
AWC	Available Water Capacity	163.9	(147.7, 184.5)
PET.thorn	Mean annual PET (Thornthwaite)	43.8	(37.3, 51.8)
PET.harg	Mean annual PET (Hargreaves)	52.6	(47.3, 59.4)
SPEI.m1	Number of month with SPEI < -1	162	(144, 178)
SPEI.m2	Number of month with SPEI < -2	13.8	(7, 22)
SPEI.q5	5% quantile of SPEI	-1.6	$(-1.6, -1.5)$
SPEI.q1	1% quantile of SPEI	-2.1	$(-2.2, -1.9)$
scPDSI.m3	Number of month with scPDSI < -3	42.6	(29, 53)
scPDSI.m4	Number of month with scPDSI < -4	9.6	(2, 14)
scPDSI.q5	5% quantile of scPDSI	-3.2	$(-3.4, -2.8)$
scPDSI.q1	1% quantile of scPDSI	-4.5	$(-4.9, -4.1)$
Late frost			
late.frost	Min temperature of the first month of the year with mean temperature > 5℃	1.7	(1.4, 2)
late.frost2	Min temperature of May	4.7	(1.5, 8.2)

Table 2: Evidence of adaptive divergence across 19 Swiss silver fir (*Abies alba* Mill.) populations using the $Q_{ST} - F_{ST}$ test of Whitlock & Guillaume (2009) and the *S*-test of Ovaskainen *et al.* (2011). 2.5%, 97.5% are the lower and upper 95% confidence intervals for Q_{ST}. The evolvability suggested by Houle (1992) was estimated using a linear mixed effects model (see Supplementary Methods S1 for details).

Trait	$Q_{ST} - F_{ST}$ test				*S*-test	Evolvability
	Q_{ST}	2.5%	97.5%	p-value	S	CV_A
Height 2013	0.18	0.05	0.42	0.003	1.00	0.100
Height 2014	0.29	0.11	0.59	0.002	1.00	0.153
Diameter 2013	0.09	0.00	0.29	0.044	0.92	0.161
Diameter 2014	0.08	0.00	0.23	0.042	0.83	0.153
Terminal Bud Break 2013	0.15	0.01	0.64	0.054	0.94	0.021
Terminal Bud Break 2014	0.18	0.04	0.57	0.025	0.86	0.021
Lateral Bud Break 2013	0.12	0.02	0.35	0.020	0.96	0.020
Maximum Growth Rate 2013	0.06	−0.02	0.28	0.133	0.67	0.184
Growth Duration 2013	0.25	0.05	0.96	0.035	0.93	0.097
Growth Cessation 2013	0.23	−2.62	2.75	0.081	0.54	0.004

Table 3: H^*-test for the first five principal components of the environmental variables listed in Table 1 for each trait. H^* and the cumulative variance explained by each PC axes are expressed as percentages. For each trait, the highest H^* value is highlighted in bold. The variables with the highest loadings on each of the PC axes are the following: PC1: bio.2 (Mean Diurnal Range) and Elevation, PC2: bio.10 (Mean Temperature of the Warmest Quarter) and PET.harg, PC3 and 4: none, PC5: bio.8 (Mean Temperature of the Warmest Quarter) and bio.15 (Precipitation seasonality)

Trait	PC1	PC2	PC3	PC4	PC5
Height 2013	92	62	35	74	41
Height 2014	94	60	33	73	42
Diameter 2013	88	45	31	66	40
Diameter 2014	78	42	29	67	45
Terminal Bud Break 2013	12	84	32	68	94
Terminal Bud Break 2014	23	82	30	35	88
Lateral Bud Break 2013	17	80	16	47	95
Maximum Growth Rate 2013	51	70	31	49	86
Growth Duration 2013	08	92	56	70	93
Growth Cessation 2013	20	73	55	33	44
Cumulative Variance	38	56	70	79	84

Figure legends

Fig. 1. (a) Geographic location of the silver fir (*Abies alba* Mill.) populations indicated by a summary of the STRUCTURE results with K=4. Each pie shows the average coancestry of the sampled, on average, 20 individuals from the 19 populations from the four assumed genetic clusters. (b) Drift distances between populations as estimated with the admixture F-model (AFM) . Coancestry between populations is the mean of the posterior means from 10 independent Markov chains. Distances were calculated from the posterior mean coancestry matrix to draw the dendrogram.

Fig. 2. (a) The strength of selection acting on a given pair of traits measured using the S statistics of Ovaskainen *et al.* (2011), and the genetic correlation between them estimated from the ancestral G-matrix (see Supplementary Methods S3 for formulae). Points and trait names in blue indicate trait pairs with genetic correlations significantly different from zero. (b) Phenotypic and genetic correlations between trait pairs estimated from the P- and the ancestral G-matrix. Points and trait names in blue indicate trait pairs with genetic correlations significantly different from zero and different from phenotypic correlations. The trait abbreviations for 2013 are as follows: H2013: Height 2013, D2013: Diameter 2013, TBB2013: Terminal Bud Break 2013, LBB2013: Lateral Bud Break 2013, MGR2013: Maximum Growth Rate 2013, GD2013: Growth Duration 2013, GC2013: Growth Cessation 2013, and with identical letter codes for 2014.

Fig. 3. Adaptive divergence for each trait separately. (a–j) Panels show the estimated ancestral additive mean trait value (horizontal line), the amount of trait divergence from this mean that is expected based on drift (gray envelop), and the estimated posterior distribution of the additive trait values for each population (boxes). Blue boxes indicate strong evidence of selection at the particular population. Populations are ordered on each panel according to their additive trait values.

Fig. 4. Correlated adaptive divergence in a two-trait space between Terminal Bud Break, Growth Duration and Maximum Growth Rate. Colors indicate the mean water use efficiency (δ^{13}C) of ten adult trees from the given population. Less negative δ^{13}C indicate higher water use efficiency. The capital letter A in the middle of the ellipses indicates the estimated ancestral additive mean trait value. Ellipses represent the median amount of trait divergence that is expected based on drift for each population (null hypothesis). Population codes (3 letters) represent the median of the posterior distribution of the additive trait values for each population. Populations with strong evidence of selection using the S-test are highlighted with an ellipse in color (identical to that of the population code). Ellipses of populations that do not deviate from drift are shown in gray.

Fig. 5. Principal component (PC) analysis of the environmental variables listed in Table 1 with populations (three letter codes) highlighted in blue if they showed evidence of selection in the S-tests for 2013 or 2014 Height (a) and for Terminal Bud Break, Maximum Growth Rate and Duration (b). Each panel shows the environmental space with the first two PC axes that had explained the highest amount of variance using the H^*-test, which were PC 1 and 4 for 2013 or 2014 Height, and PCs 2 and 5 for Bud Break and Growth Duration.

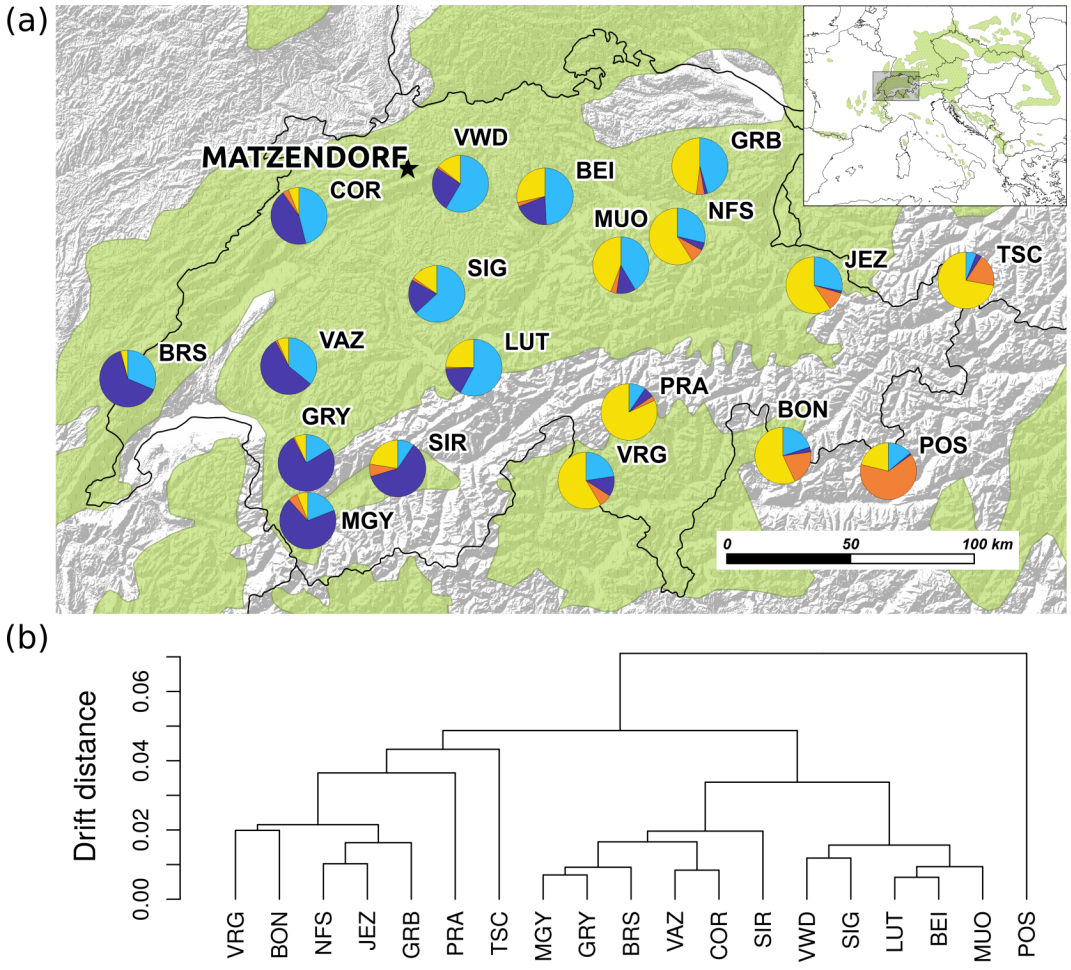
(a)
MATZENDORF
VWD
BEI
GRB
COR
MUO
NFS
SIG
JEZ
TSC
BRS
VAZ
LUT
PRA
GRY
BON
SIR
VRG
POS
MGY
0
50
100 km
(b)
Drift distance
0.00
0.02
0.04
0.06
VRG
BON
NFS
JEZ
GRB
PRA
TSC
MGY
GRY
BRS
VAZ
COR
SIR
VWD
SIG
LUT
BEI
MUO
POS

Figure 1

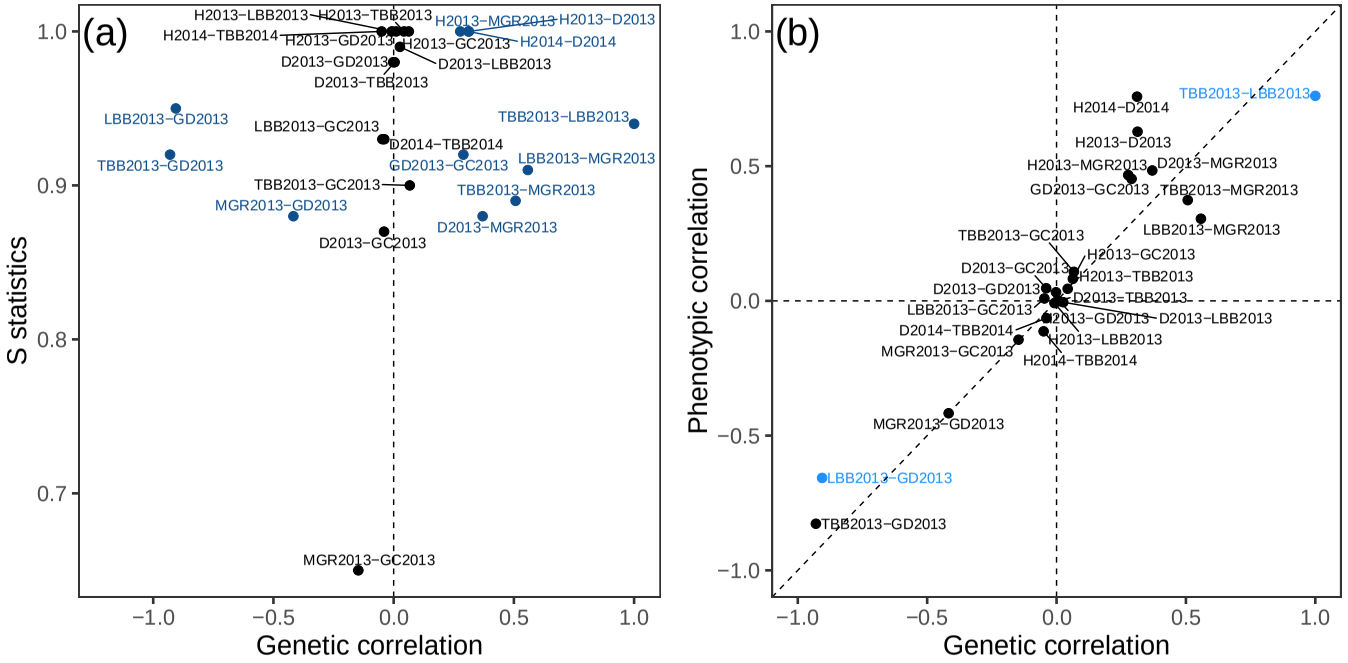
(a)
S statistics
Genetic correlation
1.0
0.9
0.8
0.7
−1.0
−0.5
0.0
0.5
1.0
H2013−LBB2013
H2013−TBB2013
H2013−MGR2013
H2013−D2013
H2014−TBB2014
H2013−GD2013
H2013−GC2013
H2014−D2014
D2013−GD2013
D2013−LBB2013
D2013−TBB2013
LBB2013−GD2013
LBB2013−GC2013
TBB2013−LBB2013
D2014−TBB2014
TBB2013−GD2013
GD2013−GC2013
LBB2013−MGR2013
TBB2013−GC2013
TBB2013−MGR2013
MGR2013−GD2013
D2013−MGR2013
D2013−GC2013
MGR2013−GC2013
(b)
Phenotypic correlation
Genetic correlation
1.0
0.5
0.0
−0.5
−1.0
TBB2013−LBB2013
H2014−D2014
H2013−D2013
H2013−MGR2013
D2013−MGR2013
GD2013−GC2013
TBB2013−MGR2013
LBB2013−MGR2013
TBB2013−GC2013
H2013−GC2013
D2013−GC2013
H2013−TBB2013
D2013−GD2013
D2013−TBB2013
LBB2013−GC2013
H2013−GD2013
D2013−LBB2013
D2014−TBB2014
H2013−LBB2013
MGR2013−GC2013
H2014−TBB2014
MGR2013−GD2013
LBB2013−GD2013
TBB2013−GD2013

Figure 2

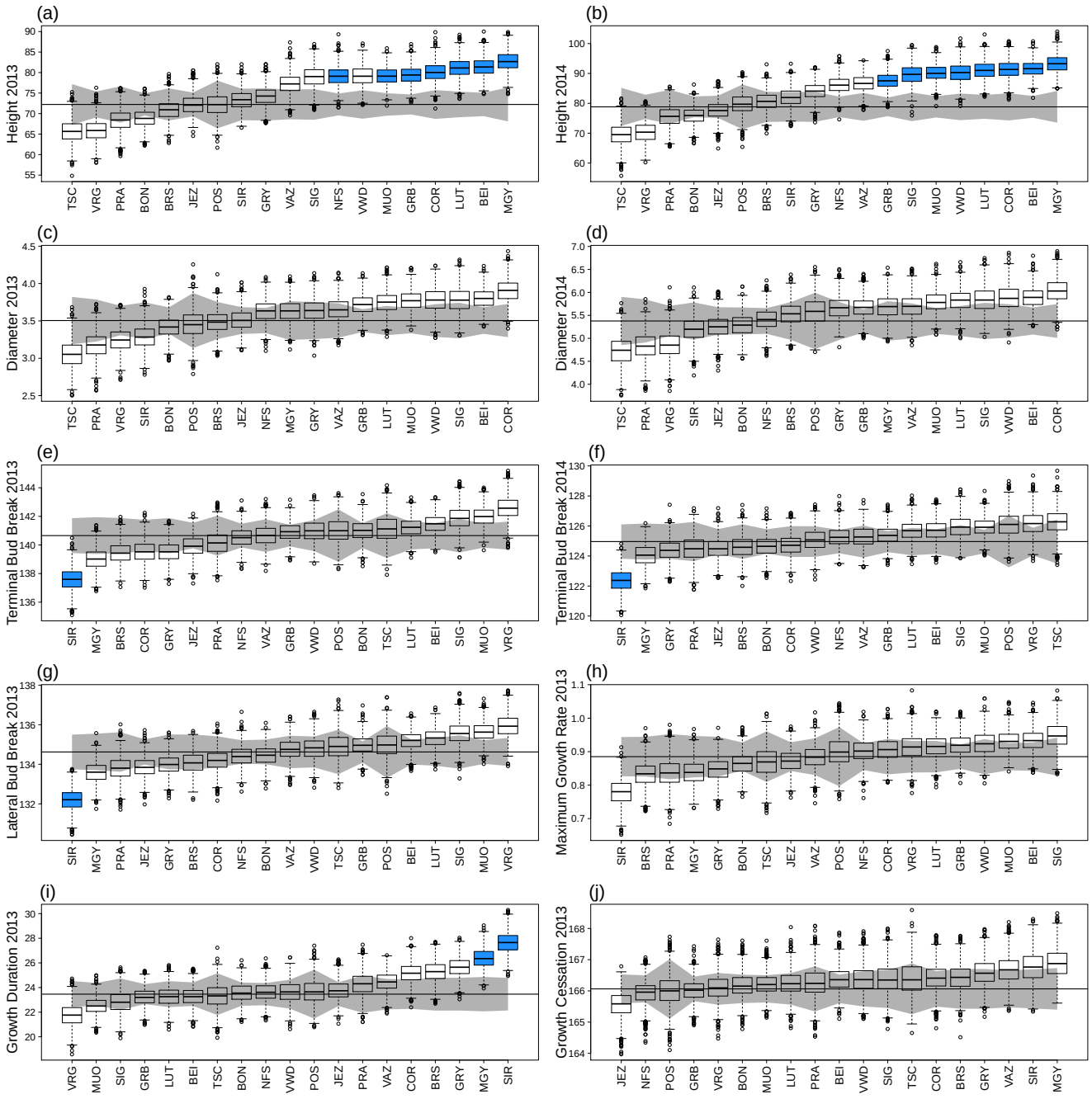
(a)
Height 2013
TSC VRG PRA BON BRS JEZ POS SIR GRY VAZ SIG NFS VWD MUO GRB COR LUT BEI MGY
(b)
Height 2014
TSC VRG PRA BON JEZ POS BRS SIR GRY NFS VAZ GRB SIG MUO VWD LUT COR BEI MGY
(c)
Diameter 2013
TSC PRA VRG SIR BON POS BRS JEZ NFS MGY GRY VAZ GRB LUT MUO VWD SIG BEI COR
(d)
Diameter 2014
TSC PRA VRG SIR JEZ BON NFS BRS POS GRY GRB MGY VAZ MUO LUT SIG VWD BEI COR
(e)
Terminal Bud Break 2013
SIR MGY BRS COR GRY JEZ PRA NFS VAZ GRB VWD POS BON TSC LUT BEI SIG MUO VRG
(f)
Terminal Bud Break 2014
SIR MGY GRY PRA JEZ BRS BON COR VWD NFS VAZ GRB LUT BEI SIG MUO POS VRG TSC
(g)
Lateral Bud Break 2013
SIR MGY PRA JEZ GRY BRS COR NFS BON VAZ VWD TSC GRB POS BEI LUT SIG MUO VRG
(h)
Maximum Growth Rate 2013
SIR BRS PRA MGY GRY BON TSC JEZ VAZ POS NFS COR VRG LUT GRB VWD MUO BEI SIG
(i)
Growth Duration 2013
VRG MUO SIG GRB LUT BEI TSC BON NFS VWD POS JEZ PRA VAZ COR BRS GRY MGY SIR
(j)
Growth Cessation 2013
JEZ NFS POS GRB VRG BON MUO LUT PRA BEI VWD SIG TSC COR BRS GRY VAZ SIR MGY

Figure 3

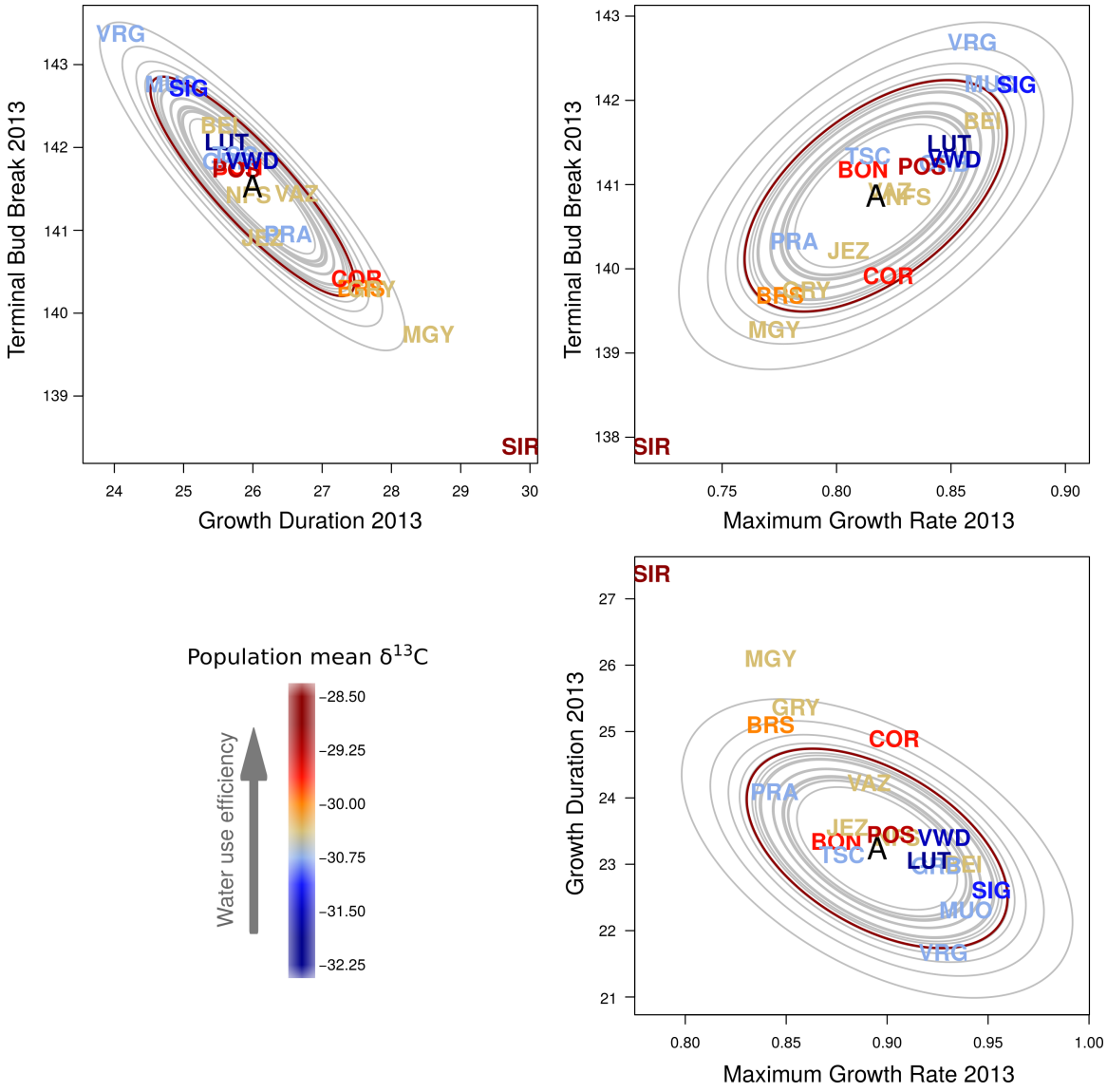
Terminal Bud Break 2013
Growth Duration 2013
Maximum Growth Rate 2013
Growth Duration 2013
Maximum Growth Rate 2013
Population mean δ13C
Water use efficiency
−28.50
−29.25
−30.00
−30.75
−31.50
−32.25
VRG
SIG
LUT
VWD
POS
A
VAZ
PRA
JEZ
COR
BRS
MGY
SIR
BON
TSC
BEI
MUO
GRY

Figure 4

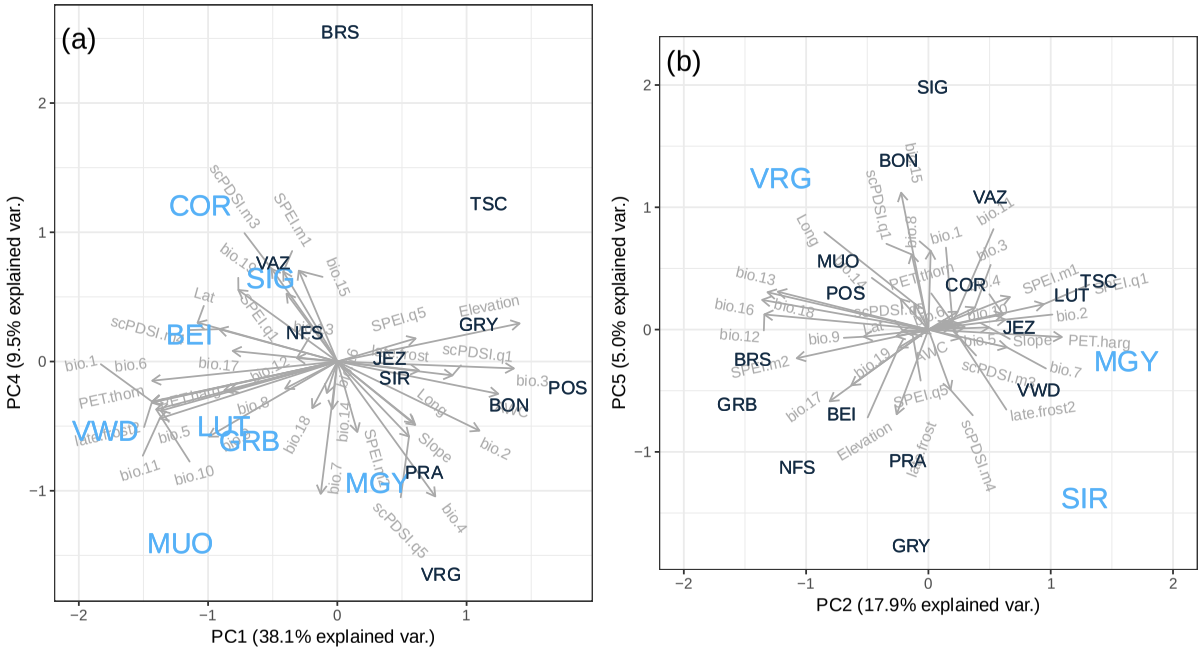
(a)
BRS
COR
TSC
VAZ
SIG
BET
NFS
GRY
JEZ
SIR
POS
BON
VWD
LUT
GRB
MGY
PRA
MUO
VRG
scPDSI.m3
SPEI.m1
SPEI.q5
Elevation
scPDSI.q1
Lat
bio.1
bio.6
bio.17
PET.thorn
bio.8
bio.5
bio.11
bio.10
bio.18
bio.14
bio.7
Slope
bio.2
bio.4
scPDSI.q5
bio.3
Long
PC4 (9.5% explained var.)
PC1 (38.1% explained var.)
(b)
SIG
VRG
BON
VAZ
MUO
COR
POS
TSC
LUT
JEZ
BRS
MGY
GRB
BEI
VWD
NFS
PRA
SIR
GRY
bio.15
scPDSI.q1
Long
bio.1
bio.3
bio.13
PET.thorn
SPEI.m1
SPEI.q1
bio.16
bio.18
bio.2
bio.12
bio.9
Lat
bio.5
Slope
PET.harg
SPEI.m2
bio.19
AWC
scPDSI.m3
bio.7
SPEI.q5
late.frost2
bio.17
Elevation
late.frost
scPDSI.m4
PC5 (5.0% explained var.)
PC2 (17.9% explained var.)

Figure 5

Supplementary Information

Title: Adaptation to local climate in a multi-trait space: evidence from silver fir (*Abies alba* Mill.) populations across a heterogeneous environment

Authors: Katalin Csilléry, Otso Ovaskainen, Christoph Sperisen, Nina Buchmann, Alex Widmer, Felix Gugerli

The following supplementary information are available for this article:

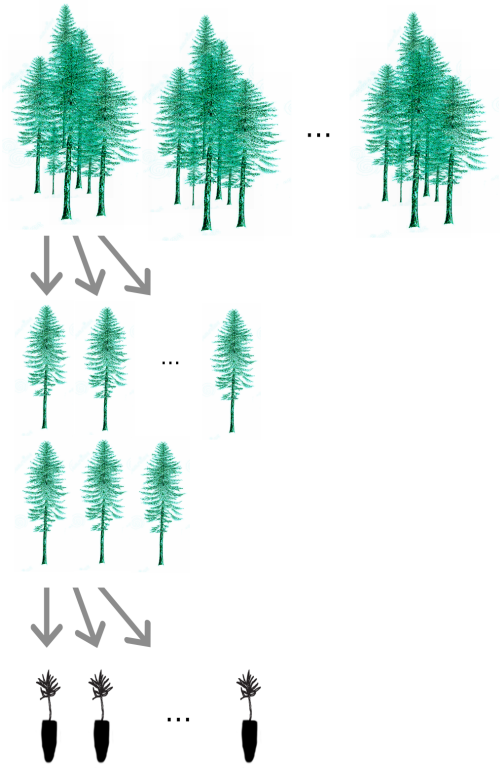

Experimental units and samples taken	Data obtained	Statistical analysis
Region Selection of 19 putatively autochthonous silver fir populations	Coarse-scale data on pastclimate Fine scale data for recent climate	Downscaling coarse scale (~55 km) past climate data to a 1 km grid scale
Population Needle samples from 20 adult trees	SNP genotypes $\delta^{13}C$	Population genetic differentiation (F_{ST}) Demographic inference: 1. coancestry matrix (AFM) 2. genetic clustering (STRUCTURE) Mean water use efficiency of populations
Mother tree Seeds from 3 mother trees (some included in the 20)	Weight of 1000 seeds (maternal effects)	Establishing the pedigree
Half-sib family ~14 seedlings grown in a common garden	Quantitative traits in the 4^{th} and 5^{th} growing season	Population differentiation in quantitative traits (Q_{ST})

Combined analysis of selection using multiple data types:

1. Q_{ST}-F_{ST} comparisons
2. Bayesian animal model to estimate additive genetic traits values and population effects while simultaneously accounting for the demography and the pedigree
3. S-test of selection in quantitative traits
3. H-test for the role of climate in trait divergence
4. Contrasting seedling trait divergence and adult mean water use efficiency

Figure S1: Schematic illustration of the work-flow.

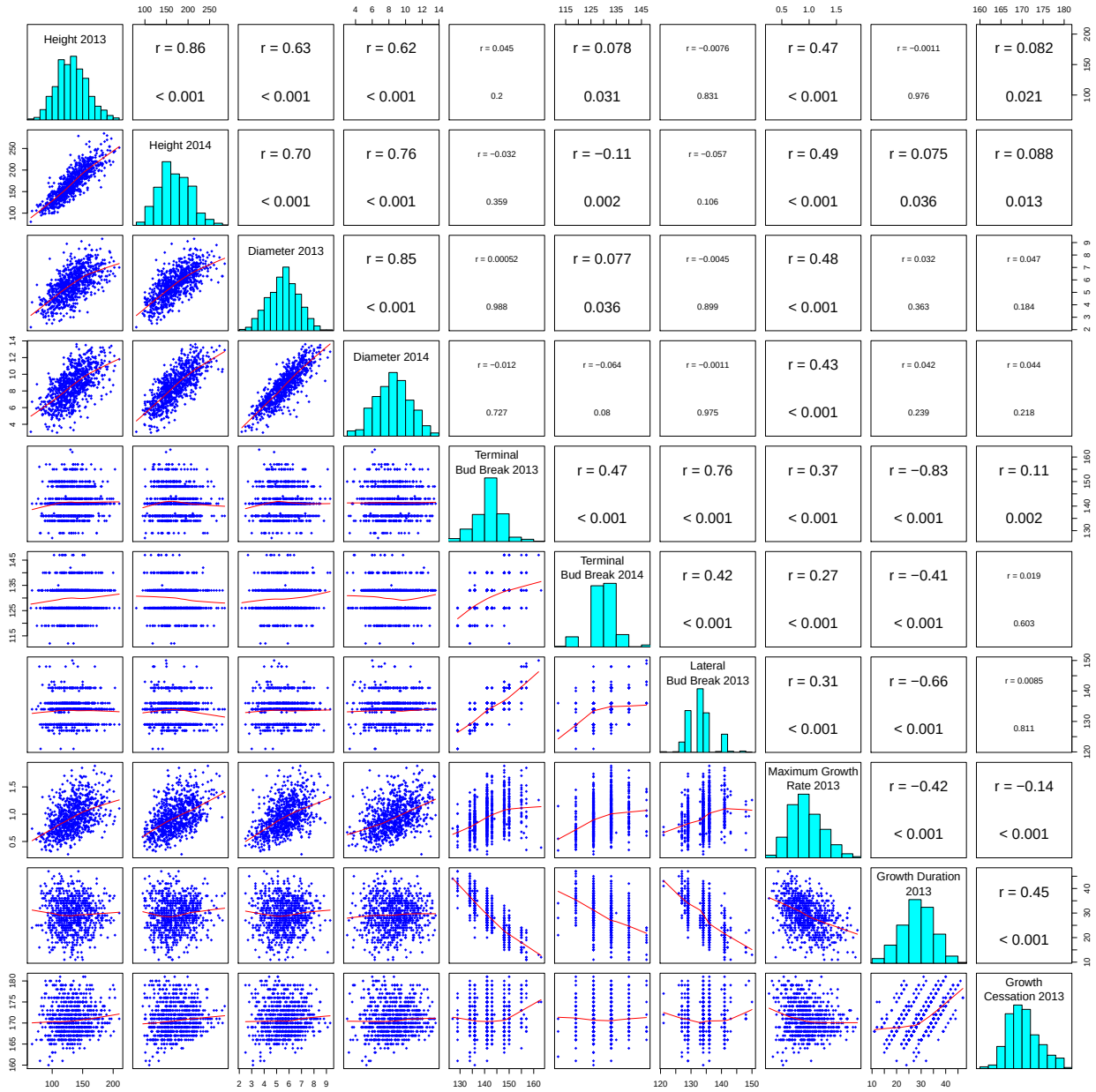

Figure S2: Raw values of traits measured in a common garden on silver fir (*Abies alba* Mill.) seedlings. Figures show scatter plots between values for all pairs of traits (lower triangle), the distribution of each trait (diagonal), and the Pearson's correlation coefficient and associated *p*-value from a correlation test between values of all pairs of traits (upper triangle).

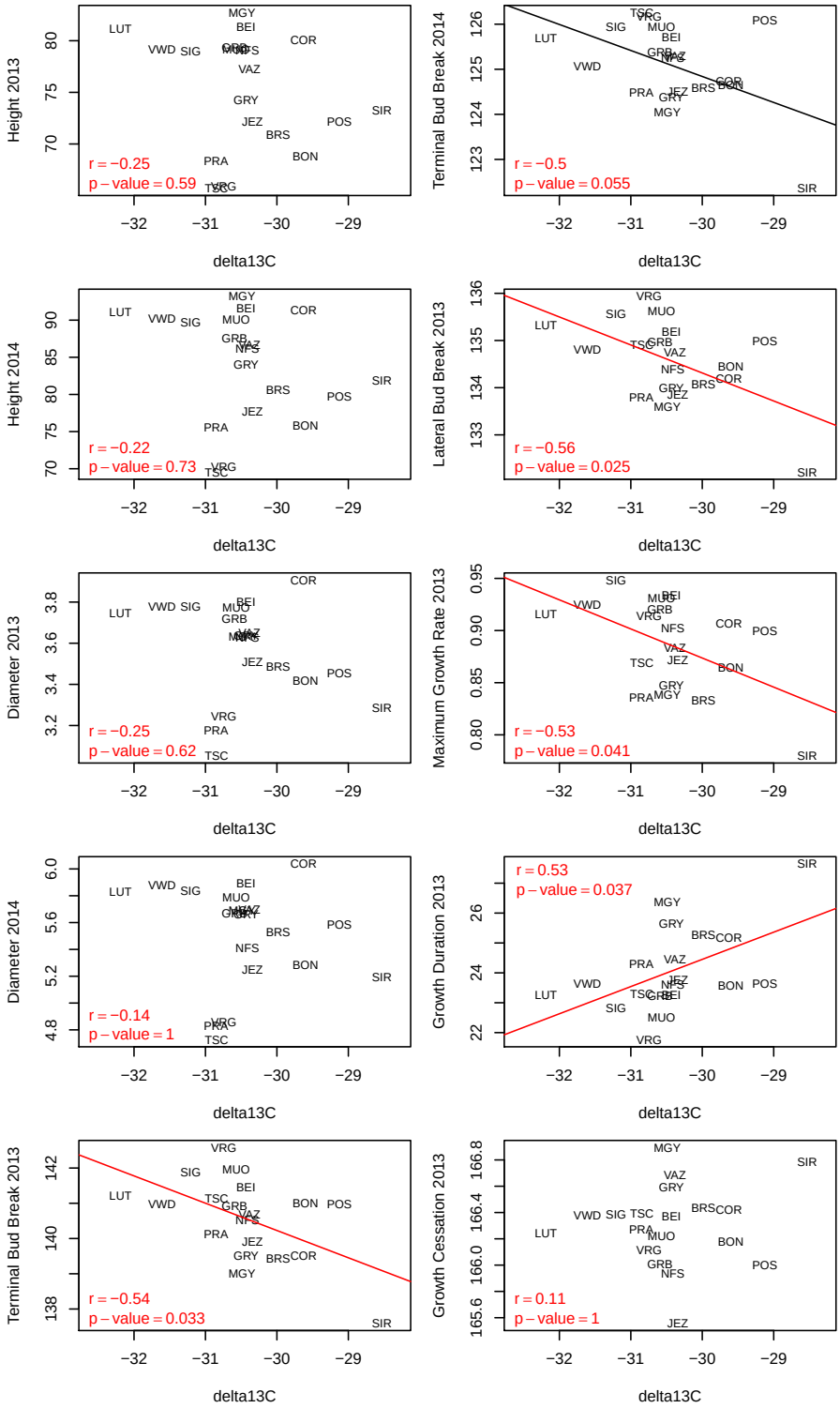

Figure S3: Correlation between population mean $\delta^{13}C$ of adult trees measured *in-situ* and the additive genetic trait values of seedlings in the ten quantitative traits. Pearson's correlation and p-values from a correlation test adjusted for multiple testing are written on each panel in red. The direction of significant correlations is indicated with a red line, while a black line indicates a marginally significant correlation.

Table S1: Abbreviations of the population names, their longitude and latitude, elevation in meters, and names of the nearby village (all in Switzerland) from which the population name abbreviations were derived. Data base/Publication/Expert specifies the source of information for deriving the putatively autochthonous status of the populations (see next page for details of abbreviations). NKS status is provided for populations present in the NKS data base.

Population code	Latitude	Longitude	Elevation	Nearby village	Data base/Publication/Expert	NKS status
BEI	47.230°*N*	8.318°*E*	843	Beinwil	Dr A. Burkhart (WSL, Researcher)/NKS	la
BON	46.324°*N*	9.541°*E*	1334	Bondo	Huss/Burga	NA
BRS	46.595°*N*	6.175°*E*	1221	Le Chenit (Le Brassus)	Huss/Burga	NA
COR	47.162°*N*	7.055°*E*	840	Cormoret	NKS	la
GRB	47.334°*N*	9.114°*E*	922	Oberhelfenschwil (Graben)	IUFRO/NKS	a
GRY	46.299°*N*	7.091°*E*	1433	Gryon	NKS	la
JEZ	46.921°*N*	9.700°*E*	1158	Jenaz	U. Bḧler (GR, Forest Office)	NA
					M. Flury (Jenaz GR, District forester)	
LUT	46.634°*N*	7.952°*E*	817	Lütschental	Burga/K. Zumbrunn (BE, Forester)	NA
MGY	46.095°*N*	7.100°*E*	1022	Martigny	C. Pernstich (VS, Forestry Office)	NA
MUO	46.991°*N*	8.708°*E*	691	Muotatal	Max Bc̈hel (Muotatal SZ, District forester)	NA
NFS	47.090°*N*	8.997°*E*	1152	Näfels	J. Walcher and	NA
					K. Winzeler (GL, Forestry Office)	
POS	46.270°*N*	10.082°*E*	1602	Poschiavo (Le Prese)	U. Bühler (GR, Forestry Office)	NA
PRA	46.479°*N*	8.750°*E*	1180	Prato (Leventina)	Huss/Burga/IUFRO	NA
SIG	46.891°*N*	7.761°*E*	938	Signau	Huss/Burga/Dr L. Walthert (WSL, Researcher)	NA
SIR	46.280°*N*	7.560°*E*	1149	Sierre	IUFRO/NKS/Huss	a
TSC	46.938°*N*	10.481°*E*	1284	Tschlin	IUFRO/NKS/Huss/Burga	a
VAZ	46.639°*N*	7.002°*E*	965	Maules	Dr L. Walthert (WSL, Researcher)	NA
VRG	46.237°*N*	8.530°*E*	1149	Vergeletto	IUFRO/NKS/Huss	la
VWD	47.273°*N*	7.884°*E*	481	Vordemwald	LWF/Huss/	NA
					Dr L. Walthert and Dr P. Weber (WSL, Researcher)	NA

NKS: Der nationale Kataster der Samenerntebestnde (National catalogue of seed sources) http://www.nks.admin.ch/
IUFRO: International Union of Forest Research Organizations
https://www.iufro.org/
LWF: Long-term Forest Ecosystem Research
https://www.wsl.ch/en/forest/forest-development-and-monitoring/long-term-forest-ecosystem-research-lwf.html
Huss: Hussendörfer, E. (1997): Untersuchungen über die genetische Variation der Weisstanne (*Abies alba* Mill.) unter dem Aspekt der In-situ-Erhaltung genetischer Ressourcen in der Schweiz (PhD thesis ETH Zurich Nr. 11849). Beih. Schweiz. Z. Forstwes. 83: 1–151 (in German)
Burga: Burga, CA and Hussendörfer, E (2001): Vegetation history of *Abies alba* Mill. (silver fir) in Switzerland–pollen analytical and genetic surveys related to aspects of vegetation history of *Picea abies* (L.) H. Karsten (Norway spruce). Vegetation History and Archaeobotany 10 (3): 151-15
WSL: Swiss Federal Research Institute WSL
a: autochthonous
la: likely autochthonous
NA: not applicable

Table S2: Principal Component Analysis (PCA) of the 36 environmental variables listed in Table 1 (main text). PC axes 1 to 5 explained 84.5% of the variance in the raw environmental variables. The first ten environmental variables with the highest loadings are shown for each PC axes.

PC1 (38.1%)		PC2 (18.0%)		PC3 (14.0%)		PC4 (9.5%)		PC5 (5.0%)	
Variables	Loadings	Variables	Loadings	Variables	Loadings	Variables	Loadings	Variables	Loadings
late.frost2	-0.26	bio.16	-0.36	Long	0.35	bio.4	-0.38	bio.15	0.56
PET.thorn	-0.26	bio.12	-0.35	bio.14	-0.33	bio.7	-0.37	late.frost	-0.35
bio.1	-0.26	bio.13	-0.35	SPEI.q5	-0.32	scPDSI.m3	0.26	bio.8	0.32
bio.6	-0.26	bio.18	-0.33	bio.8	0.24	bio.15	0.26	scPDSI.q1	0.31
Elevation	0.26	PET.harg	0.29	scPDSI.m3	0.24	SPEI.m1	0.25	bio.17	-0.29
bio.10	-0.25	SPEI.m2	-0.28	scPDSI.q5	-0.24	bio.9	-0.21	scPDSI.m4	-0.25
bio.11	-0.25	SPEI.q1	0.25	Lat	0.23	scPDSI.q5	-0.21	bio.19	-0.23
bio.3	0.25	bio.17	-0.21	bio.19	-0.21	bio.19	0.2	bio.18	0.15
bio.5	-0.25	SPEI.m1	0.18	SPEI.m1	-0.2	SPEI.m2	-0.2	bio.13	0.15
AWC	0.23	bio.7	0.17	scPDSI.q1	-0.2	bio.2	-0.19	SPEI.m1	0.13

Table S3: *S*-test, genotypic (r_g) correlations estimated from the posterior distribution of the ancestral *G*-matrix (see Results in the main text for details), phenotypic correlations (r_p), the absolute difference between the latter two (Abs. diff.), and the p-value from a standardized Mantel test that indicates if the G_A and *P*-matrices are correlated with each other. Traits were measured on silver fir (*Abies alba* Mill.) seedlings in a common garden.

Trait pair	*S*-test	r_g			r_p	Mantel-test	
		Mean	Lower 95% CI	Upper 95% CI	Mean	Abs. diff.	p-value
Height 2013-Diameter 2013	1.00	0.31	0.23	0.38	0.63	−0.32	0.000
Height 2013-Terminal Bud Break 2013	1.00	0.04	−0.09	0.15	0.04	0.00	0.023
Height 2013-Lateral Bud Break 2013	1.00	−0.01	−0.13	0.12	−0.01	0.00	0.009
Height 2013-Maximum Growth Rate 2013	1.00	0.28	0.13	0.39	0.47	−0.19	0.000
Height 2013-Growth Duration 2013	1.00	0.01	−0.08	0.11	0.00	0.01	0.026
Height 2013-Growth Cessation 2013	1.00	0.06	−0.06	0.22	0.08	−0.02	0.001
Diameter 2013-Terminal Bud Break 2013	0.98	0.00	−0.16	0.16	0.00	0.00	0.000
Diameter 2013-Lateral Bud Break 2013	0.99	0.03	−0.14	0.21	0.00	0.02	0.001
Diameter 2013-Maximum Growth Rate 2013	0.88	0.37	0.19	0.52	0.48	−0.11	0.003
Diameter 2013-Growth Duration 2013	0.98	0.00	−0.15	0.12	0.03	−0.03	0.001
Diameter 2013-Growth Cessation 2013	0.87	−0.04	−0.25	0.18	0.05	−0.01	0.059
Terminal Bud Break 2013-Lateral Bud Break 2013	0.94	1.00	1.00	1.55	0.76	0.55	0.557
Terminal Bud Break 2013-Maximum Growth Rate 2013	0.89	0.51	0.16	0.84	0.37	0.13	0.000
Terminal Bud Break 2013-Growth Duration 2013	0.92	−0.93	−1.09	−0.68	−0.83	0.10	0.000
Terminal Bud Break 2013-Growth Cessation 2013	0.90	0.07	−0.25	0.38	0.11	−0.04	0.104
Lateral Bud Break 2013-Maximum Growth Rate 2013	0.91	0.56	0.25	0.86	0.30	0.25	0.002
Lateral Bud Break 2013-Growth Duration 2013	0.95	−0.91	−1.10	−0.66	−0.66	0.25	0.063
Lateral Bud Break 2013-Growth Cessation 2013	0.93	−0.05	−0.38	0.30	0.01	0.04	0.516
Maximum Growth Rate 2013-Growth Duration 2013	0.88	−0.42	−0.61	−0.20	−0.42	0.00	0.000
Maximum Growth Rate 2013-Growth Cessation 2013	0.65	−0.15	−0.48	0.24	−0.14	0.00	0.001
Growth Duration 2013-Growth Cessation 2013	0.92	0.29	0.03	0.53	0.45	−0.16	0.037
Height 2014-Diameter 2014	1.00	0.31	0.23	0.37	0.76	−0.45	0.000
Height 2014-Terminal Bud Break 2014	1.00	−0.05	−0.13	0.04	−0.11	−0.06	0.010
Diameter 2014-Terminal Bud Break 2014	0.93	−0.04	−0.20	0.14	−0.06	−0.02	0.000

Supplementary Methods S1: Estimating of the heritability, evolutionary potential and population differentiation across the 19 populations: the effect of experimental design, covariates, sample size and scaling

Effect of nursery design on quantitative genetic parameters

The full common garden study of (Frank *et al.*, 2017) consisted of 4107 observations on 91 populations and 259 families. The subset analyzed in this paper, for which genetic marker and water use efficiency data had been collected consisted of 880 observations on 19 populations and 57 families. Seedlings were planted in seven nursery beds each with 47 row pairs. Provenances were planted in the order of reading rows of an imaginary grid placed on the map of Switzerland from the top left to right bottom corner. The three families were planted one after the other, each taking up two rows. Size, growth and phenology traits were not measured in the nursery. Height and Diameter were first measured in 2012 after the transplantation to the common garden site, thus these measures may also incorporate differing planting depth. In contrast, the weight of 1000 seeds were measured for each family, which provides means of accounting for maternal effects.

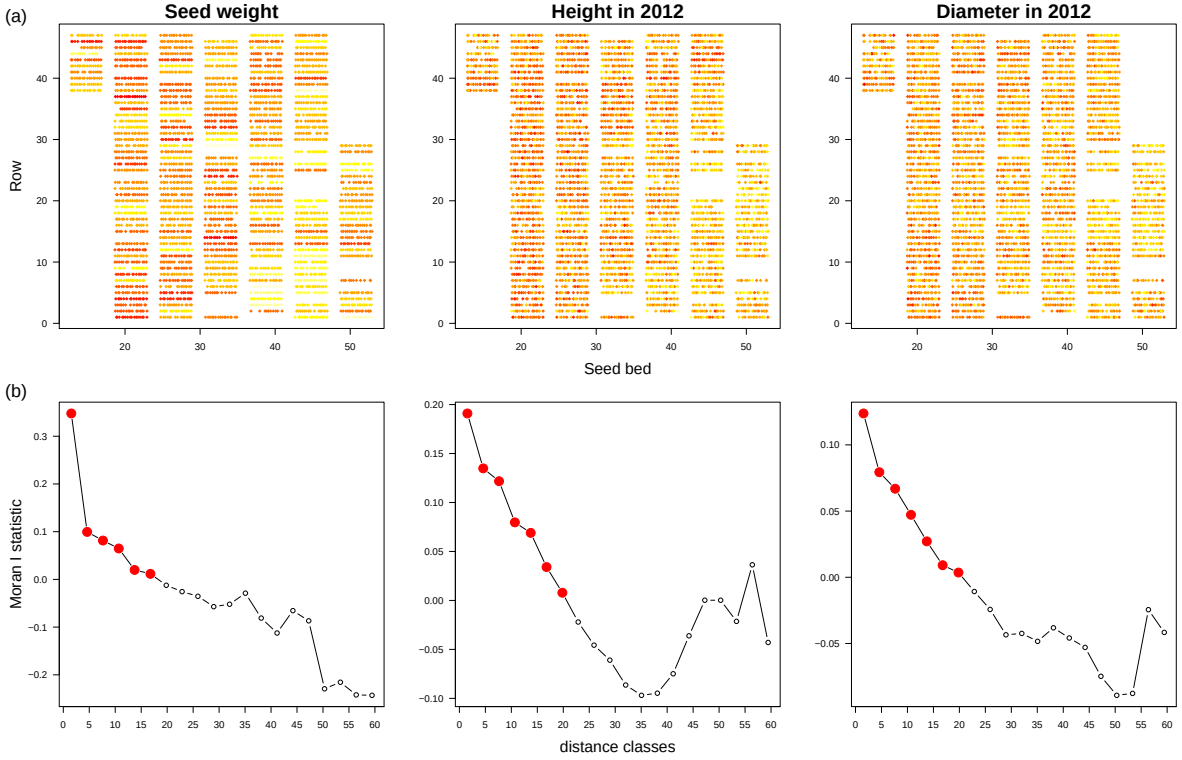

Figure A1: (a) Spatial patterns in Seed Weight, Height 2012 and Diameter 2012 in the nursery. x (seed bed) and y (row) coordinates correspond to distances in meters. The 94 rows are illustrated by 47 row-pairs that the three families of a population occupied. Colors reflect the absolute values of each variable with larger values being darker red. (b) Spatial autocorrelation with respect to the spatial arrangement in the nursery expressed with Moran's I. Red dots indicate significant clustering of similar values.

Fig. A1(a) shows maps of the nursery beds with colors proportional to Seed Weight (trait names are capitalized hereafter), and seedling's Height and Diameter 2012 and the degree of

spatial autocorrelation (Fig. A1(b)). Although there is clear evidence for spatial autocorrelation in Height and Diameter 2012 related to the spatial arrangement in the nursery (Fig. A1), we argue that this is entirely due to population and family effects that were non-randomized. The two lines of evidence to support this are: (i) the presence of spatial autocorrelation with respect to spatial arrangement in the nursery is present already for Seed Weight, and (ii) the lack of spatial correlation other than the effects of population and family for Height 2012 (Table A1). Thus, we conclude that it is likely that the non-randomization of populations and families did not alter the consecutive trait measures. Yet, including Seed Weight as a covariate in models of 2013 and 2014 traits seems useful because it potentially accounts for maternal effects.

Frank *et al.* (2017) used Height 2012 as a covariate to account for nursery effects when estimating population and family variance components for all traits measured in 2013 and 2014. Height 2012 is strongly correlated with Height 2013 (Pearson's correlation of r=0.85), thus including it as a covariate, does not account for the temporal correlation due to repeated measures for Height. Thus, including Height 2012 as a covariate decreased the population and family variance components for Height and Diameter 2013 and Growth variables, while leaving the phenology traits unaffected (Fig. A2(a)). Thus, we did not follow the statistical treatment used in Frank *et al.* (2017).

Effect of sample size on quantitative genetic parameters

First, we assessed the effect of reduced sample size, i.e. using a subset of 19 populations out of the 91. We were interested if quantitative genetic parameters were sensitive to number of populations used, in other words, if they represent similar amounts of trait variation than the larger sample. Population genetic parameters estimated using the reduced set were overall similar to those obtained using the larger data set (Fig. A2(b)). CV_A was the most robust sample size, while Q_{ST} estimates were generally larger, which was expected given that we selected a subset of populations representing diverse ecological conditions. The ordering of the traits in terms of h^2 and Q_{ST} were also different, which most likely reflects the choice of particular populations.

Second, we assessed the effect of having only three families per population, which is the bear minimum for estimating population genetic differentiation. The low number of families also affected the study of Frank *et al.* (2017), however, they partly compensated for it by having a large number of populations (so-called "genecological" approach). We used the full data set of 91 populations to "borrow" families from nearby populations, thereby increase the number of families. We select populations that are nearby our 19 populations taking into account the following criteria: populations had to be no further than 35 km from each other, they had to be in same valley or in the neighbouring valley with the same exposition, and had to have no

Table A1: Model comparison of mixed effects models fitted with lme in R with family nested in population as random effects and with and without Seed Weight as a covariate and with and without spatial autocorrelation structure (SpAC).

Seed Weight	SpAC	df	AIC	BIC	logLik	Ratio	p-value
no	no	4	32840	32865	−16416		
no	yes	6	32843	32881	−16416	1	0.700
yes	no	5	32796	32827	−16393		
yes	yes	7	32799	32843	−16393	1	0.677

more than 200 m difference in elevation. According to these criteria, we were able to increase the number of families in 9 populations, so that the average number of families was 5.3 (range: 3-12). Our analysis showed that the resulting parameter estimates were extremely similar for all three parameters to those obtained with three families only (Fig. A2(c)).

Is the additive genetic variance homogeneous across populations?

Estimating the additive genetic variance from populations across a heterogeneous landscape involves the assumption that the additive genetic variance is constant across the sampling area. Indeed, the global population parameters presented on Fig. A2(a), and thus the results presented in Frank *et al.* (2017), assume a common additive genetic variance across Switzerland. In order to test if such an assumption is reasonable, we estimated two standardized measures of the additive genetic variance, h^2 and CV_A, for the main geographic regions of Switzerland separately using the full data set of 91 populations.

Switzerland is divided into six main forestry regions based on a phylogeographic study (Burga & Hussendörfer, 2001). We pooled these regions to three regions to assure that each region have a sample size of at least 880 to make it comparable with our study using 19 populations. As a result, the three regions had 1247 (Plateau), 1699 (Alps), and 884 (South) observations. We found that h^2 and CV_A were relatively consistent across regions (Fig. A3). Not surprisingly, CV_A was more consistent across regions than h^2 because the latter is dependent on the environmental variance, which is likely different among the regions. These results suggest that regardless of the different demographic history and potential lack of gene flow between the regions separated by high mountain passes, the additive genetic variance is of similar magnitude across the landscape across the different traits.

In conclusion, assessment of the effect of geographic region and sample size highlights that assuming a common additive genetic variance across either 90 or 19 populations without accounting for their demography and potentially differing selection pressures stays relatively robust, but not free from potential biases. Overall CV_A was more stable with respect to sample size, family number and region. Thus, in agreement with Houle (1992), Hansen *et al.* (2011), the mean standardized measure of the additive genetic variance seems more appropriate as a measure of the evolutionary potential and for comparative purposes.

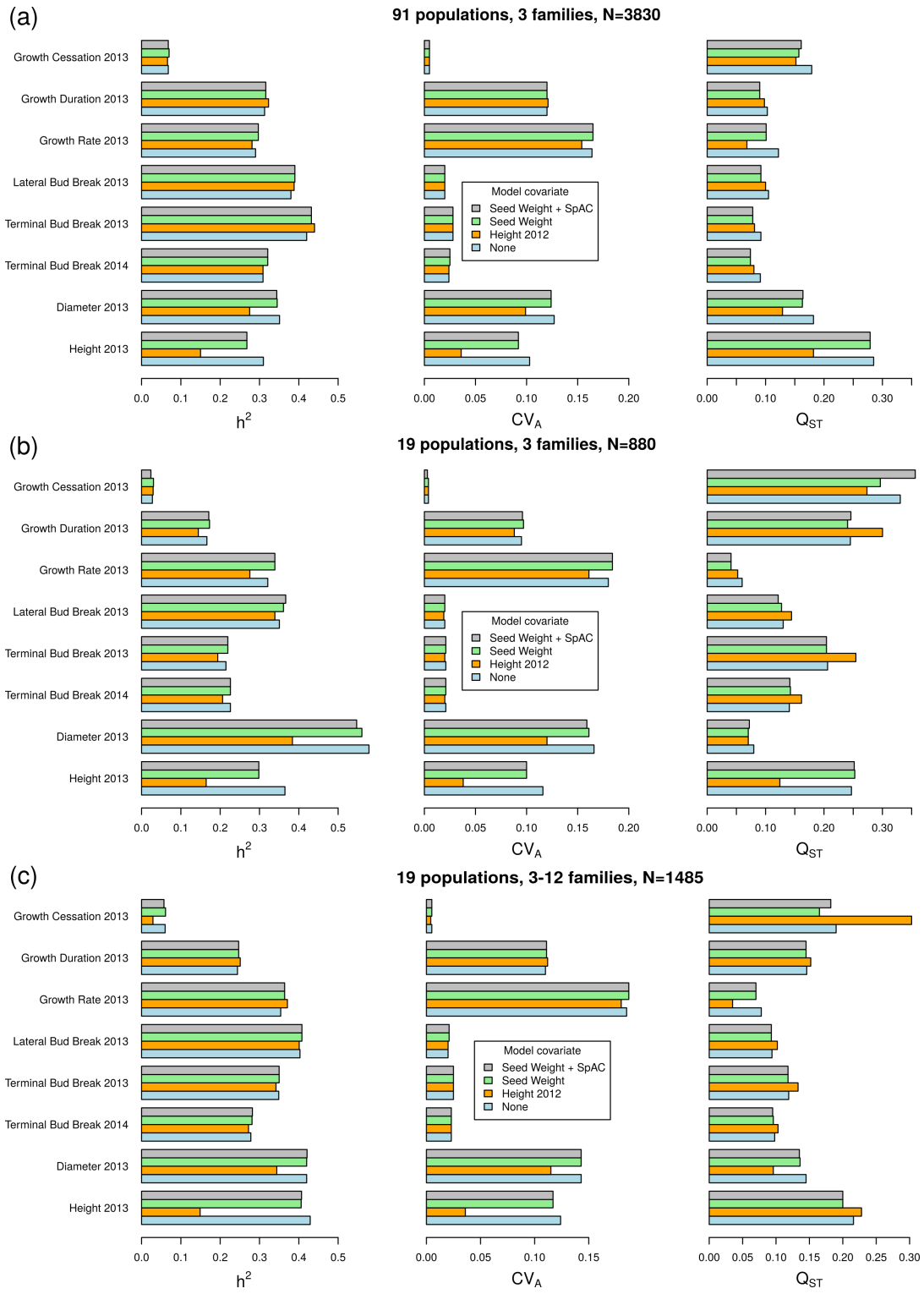

Figure A2: Heritability (h^2), additive genetic coefficient of variation (CV_A) and genetic differentiation between populations (Q_{ST}) estimated using four different versions of a mixed effects model fitted with lme in R with family nested in population as random effects and block in the common garden as fixed effect, and covariates as indicated in the legend. SpAC stands for spatial autocorrelation structure. The model with covariate Height 2012 was used in Frank *et al.* (2017). (a) using the full data set from Frank *et al.* (2017); (b) using the 19 populations studied herein; (c) using the 19 populations studied herein, but with increasing the number of families per population by pooling nearby populations.

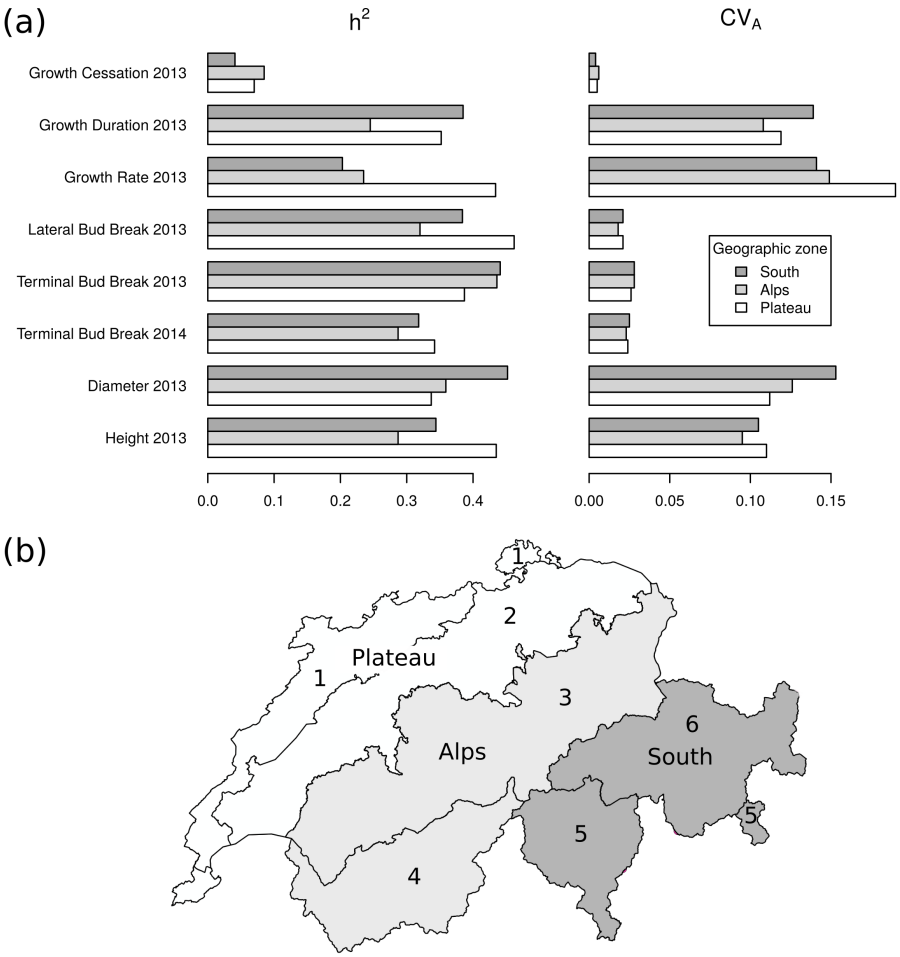

Figure A3: (a) h^2 and CV_A estimated using only the populations from one of the three main geographic regions of Switzerland. (a) The six forestry regions of Switzerland are indicated by numbers (1: Jura, 2: Plateau, 3: Alps, 4: Valley, 5: Ticino, 6: Grison). We pooled these six regions to three to have at least 800 observations for each region. The names of three regions are labelled and marked with different colours. The matching colour coding of (a) and (b) helps the reader.

Supplementary Methods S2: Estimating the demography of the 19 silver fir populations

Estimating the demography of 19 populations is a high dimensional estimation problem. We used the admixture F model (AFM), which assumes that the current populations are derived from a single, non-sampled, ancestral population (Karhunen & Ovaskainen, 2012). The method of (Ovaskainen *et al.*, 2011) also relies on this assumption. For parameter estimation, a Metropolis-Hastings algorithm is implemented in the R package RAFM (Karhunen & Ovaskainen, 2012). We ran ten independent Markov chains of the AFM model using a burn-in of 30,000 iterations followed by 10,000 iterations for estimation with a thinning interval of ten. The estimated posterior distribution of the coancestry matrix is 19 by 19, and it is challenging to use directly this matrix for convergence diagnostics. Thus, we calculated the F_{ST} from each matrix to calculate the convergence diagnostics using the R package *coda* (Fig. A4). Single chain diagnostics indicated satisfactory convergence (Table A2). All chains passed Heidelberger's test (Heidelberger & Welch, 1981). Geweke's statistics were calculated using the default window sizes, 0.1 and 0.5. We found that z-scores were between -1.96 and 1.96, indicating convergence (Geweke, 1991).

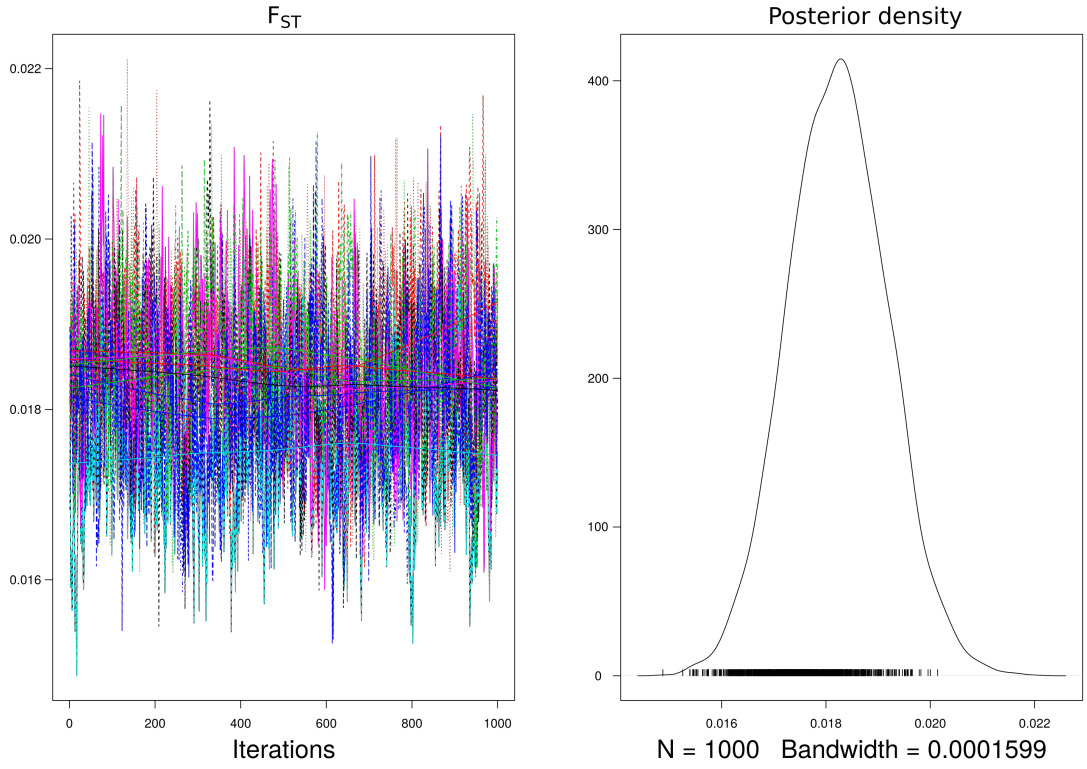

Figure A4: The posterior distribution of F_{ST} calculated from the posterior distribution of the 19 by 19 coancestry matrix across ten independent chains of the Metropolis-Hastings algorithm.

Mixing of the chains was assessed using Gelman's mean potential scale reduction factor (Gelman & Rubin, 1992). A value of one indicate that the variance between and within chains is equal. Different Markov chains reached slightly different optima, in particular, two chains had a lower F_{ST} than the others (Fig. A4 and A5). The mean potential scale factor was 1.09, with an upper credible interval of 1.19. Thus, we estimated the posterior mean coancestry matrix from each Markov chain and averaged them across the ten Markov chains.

Table A2: Single chain convergence diagnostics. The posterior distribution of F_{ST} was calculated from the posterior distribution of the 19 by 19 coancestry matrix across ten independent chains of the Metropolis-Hastings algorithm.

Chain	Heidelberger and Welch		Geweke
	result	p-value	z-score
1	passed	0.63	−1.21
2	passed	0.30	0.25
3	passed	0.74	0.53
4	passed	0.78	1.07
5	passed	0.63	−1.21
6	passed	0.05	1.81
7	passed	0.22	1.31
8	passed	0.78	−0.37
9	passed	0.50	−0.67
10	passed	0.09	0.86

To further validate the results of the AFM model, we compared it to the Bayesian clustering algorithm implemented in STRUCTURE v.2.3.4 Pritchard *et al.* (2000). We used the admixture model with correlated allele frequencies Falush *et al.* (2003), which is the closest model to AFM. Further, we included sampling location information to improve clustering performance ("locprior model", Hubisz *et al.* (2009)), an additional information that cannot be accounted for in AFM. We estimated the prior population allele frequency parameter (λ) from the data, as the default of 1 is not necessarily a good choice for SNP data, where most minor alleles are rare. We estimated λ using K = 1 to avoid non-identifiability issues with the other hyper-parameters (λ, α, F). λ was consistently around 0.65 across ten repeated runs (range: 0.63-0.66, median: 0.65). Then, we tested K values from 1 to 19 using ten independent Markov chains for each K, and 500,000 burn-in iterations and 500,000 iterations for estimation of the membership coefficients. Different number of clusters (K) were compared with Structure Harvester (Earl *et al.*, 2012) using the $LnPr(X|K)$ and Evanno *et al.*'s (2005) method. Admixture coefficients were averaged across ten repeated runs using CLUMPP v.1.1.2 Jakobsson & Rosenberg (2007) using the Greedy algorithm for any K>3 and large-K-Greedy for K>5.

STRUCTURE and AFM results were compared for each K using a Mantel test using the *ecodist* R package (Goslee & Urban, 2007). We calculated a distance matrix from the coancestry matrix and compared to a distance matrix calculated from the CLUMPP outfiles for each K. The individual coancestries of the CLUMPP outfiles were first reduced to population coancestries by taking the mean coancestry of the individuals within a population for each K yielding a 19 $\times$ K matrix for $K = 2, \therefore, 19$. Dendrograms from AFM and STRUCTURE were also compared visually using the R package *dendextend* (Galili, 2015).

The software STRUCTURE using the log likelihood criteria suggested five as optimal number of clusters, nevertheless, additional increase in the log likelihood is suggestive of deeper hierarchical structure (Figure A6). The highest similarity between AFM and STRUCTURE was achieved for $K = 4$ (Figure A7 and A8). STRUCTURE also generally confirmed the East-West differentiation as first level structure and several parts of the dendrograms from the two algorithms were identical (Figure A8). For comparison, the mean Mantel statistic between all pairs of coancestry matrices from the ten independent chains was 0.928 (range: 0.854 - 1). Thus, on average, the ten different AFM chains were more

similar to each other than AFM to STRUCTURE, there were AFM chains just as similar to each other as AFM to STRUCTURE.

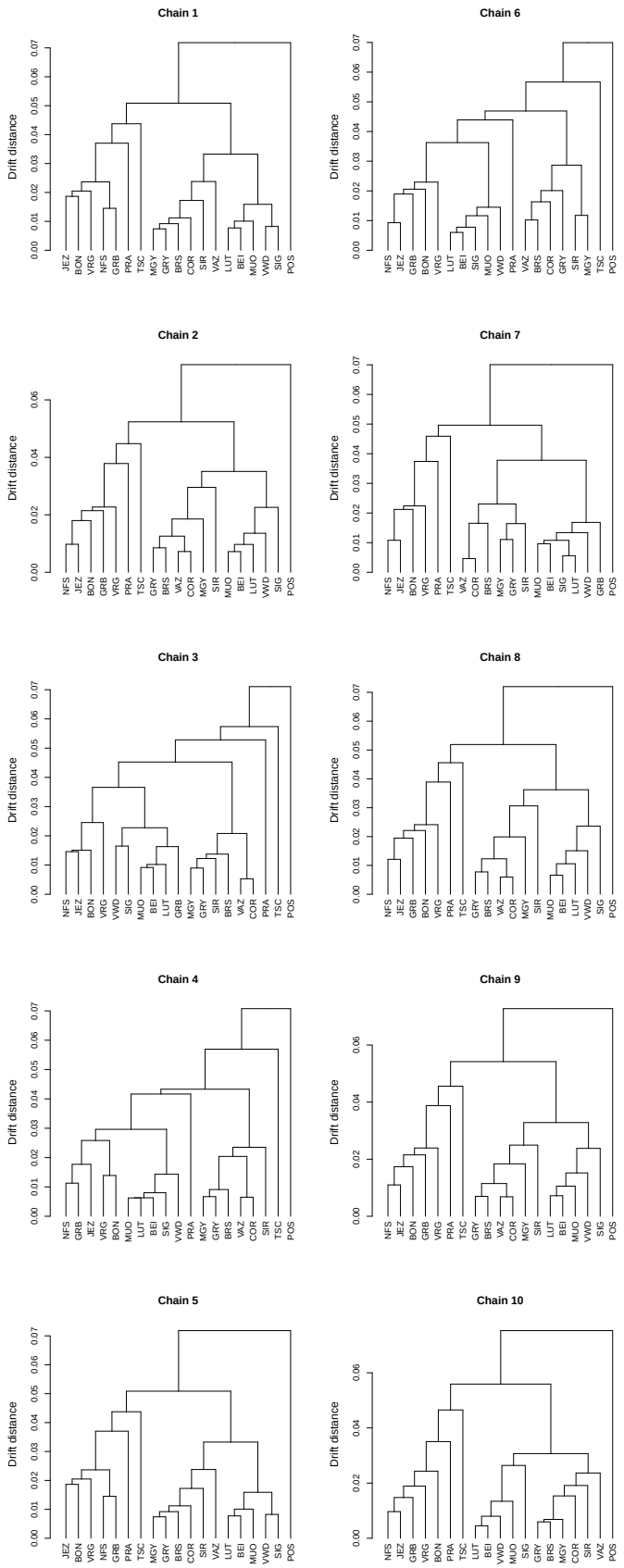

Figure A5: Drift distances between populations estimated using ten independent Markov chains of the AFM model. Each panel corresponds to a Markov chain. Distances were calculated from the posterior mean coancestry matrix to draw the dendrogram. Note that the final coancestry between populations used for inference of adaptive divergence in the main text was the mean of the posterior means from ten independent Markov chains.

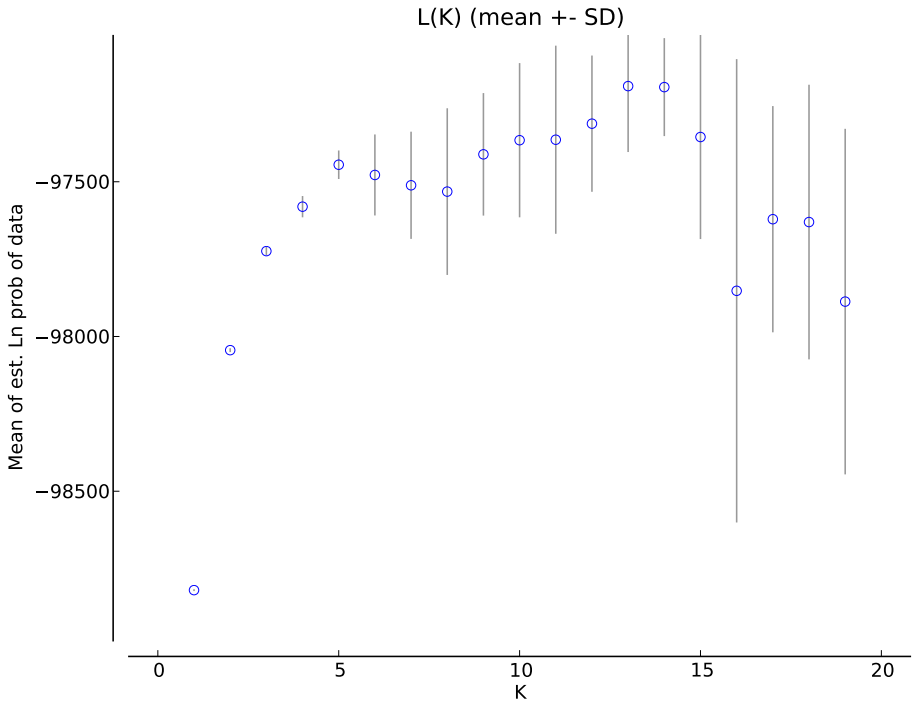

Figure A6: The log-likelihood from STRUCTURE from $K = 2$ to 19.

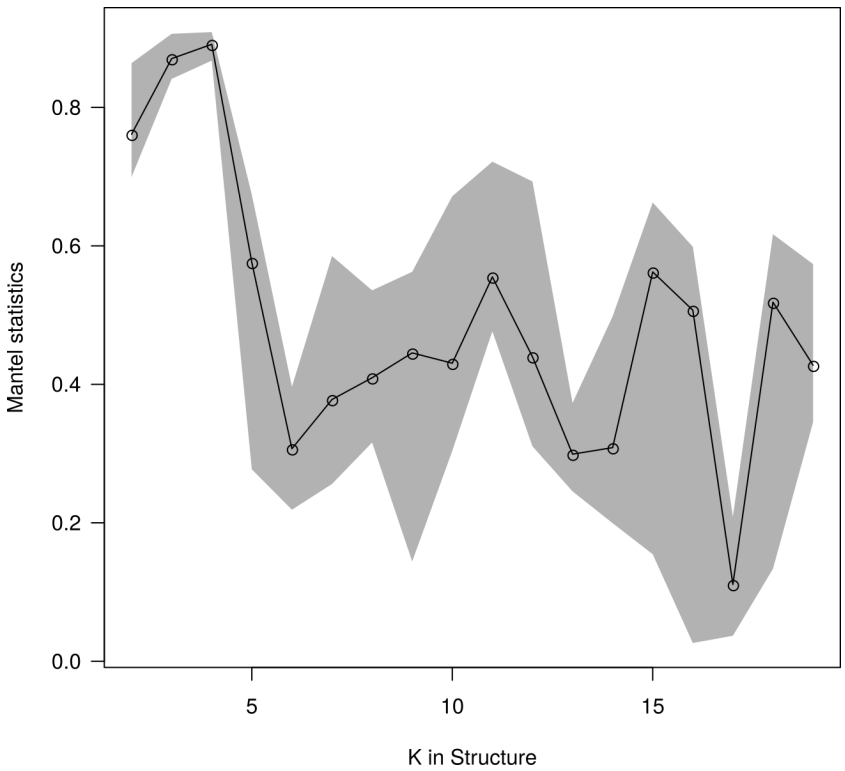

Figure A7: Mantel test statistic and its 95% percentile interval from a randomization procedure between distance matrices from AFM and STRUCTURE from $K = 2$ to 19.

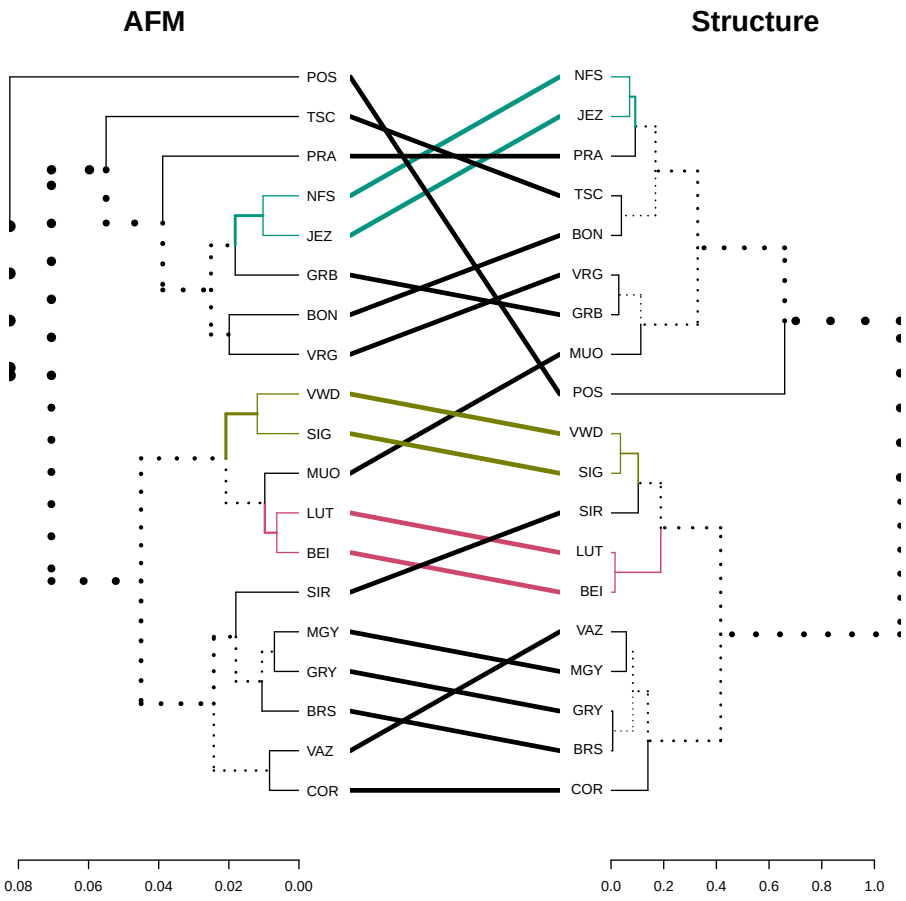

Figure A8: Entangled dendrograms from AFM and STRUCTURE with $K = 4$. Colors highlight populations that belong to the same clusters.

Supplementary Methods S3: Details of the modifications to the methods proposed by Ovaskainen *et al.* (2011) and Karhunen *et al.* (2014)

Following the notation of Ovaskainen *et al.* (2011), if we consider only additive effects, the vector of additive values of all traits for individual i is $\mathbf{a}_i$, and the matrix of additive vectors for all individuals is $\mathbf{A} = (\mathbf{a}_i)_i$. Then, the mean additive value of population X, $\mathbf{a}_X^P$, can be obtained as the mean of the additive values of all individuals in population X, and the matrix of additive vectors for all populations is $\mathbf{A}^P = (\mathbf{a}_X^P)_X$. When populations are derived from a common ancestral population and the trait values are normally distributed, under drift, the matrix of population-level effects, $\mathbf{A}^P$, is expected to follow the multivariate normal distribution as

$$\mathbf{A}^P \sim N(\boldsymbol{\mu} \otimes \mathbf{I}_{n_P}, 2\mathbf{G}^A \otimes \boldsymbol{\theta}^P), \tag{1}$$

where $\boldsymbol{\mu}$ is the vector of expected additive trait means determined by the allele frequencies in the ancestral population, n_P is the number of populations and $\mathbf{I}_{n_P}$ is an $n_P \times n_P$ identity matrix, $\mathbf{G}^A$ is the ancestral variance-covariance matrix, $\boldsymbol{\theta}^P$ is the population-to-population coancestry matrix, and $\otimes$ is the Kroenecker product. $\boldsymbol{\theta}^P$ can be estimated assuming the admixture F-model, while $\boldsymbol{\mu}$, $\mathbf{A}^P$, and $\mathbf{G}^A$ can be co-estimated using the Bayesian mixed-effects animal model accounting for the family structure of the common garden (i.e. the pedigree) and $\boldsymbol{\theta}^P$ (Ovaskainen *et al.*, 2011). Then, the additive genetic variance-covariance matrix of the contemporary populations assuming no selection, $\mathbf{G}$, can be estimated as $\mathbf{G} = 2\mathbf{G}^A(1 - \theta^S)$, where θ^S is the mean within-population (or self) coancestry of all populations, thus the drift distance of the contemporary populations from the ancestral population. Here, we estimated the heritability of traits and the genetic correlation between trait pairs as the proportion of the observed phenotypic variance and covariances that are additive (i.e. using $\mathbf{G}$) (Falconer & Mackay, 1996). The evidence for selection can be summarized using the S-statistic calculated as the Mahalanobis distance between $\mathbf{A}^P$ and the distribution of equation 1. $S = 0.5$ indicates consistency with neutrality, $S = 0$ implies a match with purifying, and $S = 1$ with diversifying selection. Thus, S measures the overall signature of selection across all populations.

In this study, we assess to what extent the particular populations deviate from their neutral expectation. Population X, whose 95% of the posterior distribution of $\mathbf{a}_X^P$ is outside of the neutral envelop defined as $\boldsymbol{\mu} \pm \sqrt{2\mathbf{G}^A \boldsymbol{\theta}_X^S}$ strongly contributes to the overall selection signal captured by the S statistic. The neutral envelop can be uni- or multi-variate depending if one or multiple traits are studied. Our motivation for this population-wise evaluation of divergence is that a single S-statistic cannot distinguish between the two scenarios of many populations that are slightly diverged or a single/few populations that are diverged to a great extent.

The H-statistics measure if the distance between the populations' mean additive trait values is more similar to the environmental distances than expected based on drift (Karhunen *et al.*, 2014). The original H-test is based on the Mantel test statistic, i.e. the product moment between the distance matrices of environment and traits. As the covariance is not only influenced by the correlation between the matrices but also by the absolute values of trait differences, the original H-test may yield false positive results. In particular, in cases with strong evidence for selection, the H statistic can be high (i.e. close to 1) even when selection is uncorrelated with the tested environmental driver (Fig. A9). For this reason, we propose the use of the H^* statistic, which is the Pearson or standardized Mantel statistic,

thus the H^*-test can be viewed as a standardized version of the H-test. We note that the superiority of a standardized Mantel statistic has already been pointed out in the context of spatial distance matrices (Legendre & Fortin, 2010).

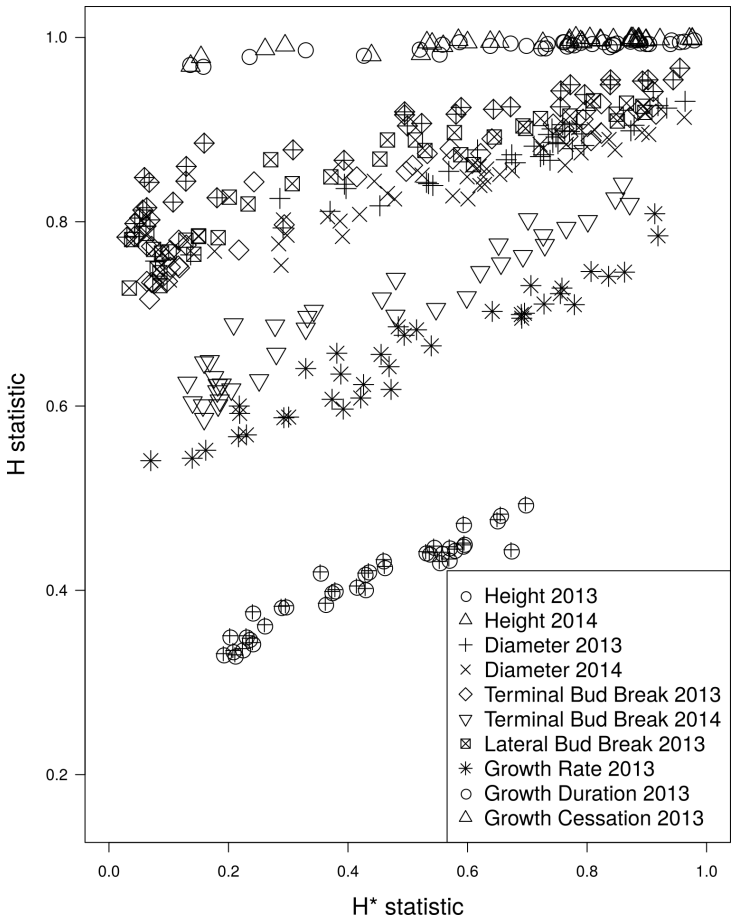

Figure A9: Comparison of the H- and H^*-statistics for the 10 studied traits. Each point indicates the H- and H^*-statistics for one of the environmental variable listed in Table 1 of the main text.

References

Burga CA, Hussendörfer E (2001) Vegetation history of *Abies alba* Mill. (silver fir) in Switzerland–pollen analytical and genetic surveys related to aspects of vegetation history of *Picea abies* (L.) H. Karsten (Norway spruce). *Veg Hist Archaeobot*, **10**: 151–159.

Earl DA, *et al.* (2012) STRUCTURE HARVESTER: a website and program for visualizing STRUCTURE output and implementing the Evanno method. *Conserv Genet Resour*, **4**: 359–361.

Evanno G, Regnaut S, Goudet J (2005) Detecting the number of clusters of individuals using the software structure: a simulation study. *Mol Ecol*, **14**: 2611–2620.

Falconer DS, Mackay TFC (1996) *Introduction to Quantitative Genetics*. Longmans Green, Harlow, Essex, UK, 4 edn.

Falush D, Stephens M, Pritchard JK (2003) Inference of population structure using multilocus genotype data: linked loci and correlated allele frequencies. *Genetics*, **164**: 1567–1587.

Frank A, Sperisen C, Howe GT, Brang P, Walthert L, Clair JBS, Heiri C (2017) Distinct genecological patterns in seedlings of Norway spruce and silver fir from a mountainous landscape. *Ecology*, **98**: 211–227.

Galili T (2015) dendextend: an r package for visualizing, adjusting, and comparing trees of hierarchical clustering. *Bioinformatics*, **31**: 3718–3720.

Gelman A, Rubin DB (1992) Inference from iterative simulation using multiple sequences. *Stat Sci*, **7**: 457–511.

Geweke J (1991) Evaluating the accuracy of sampling-based approaches to calculating posterior moments. In: *Bayesian Statistics 4* (eds. Bernado J, Berger J, Dawid A, Smith A). Clarendon Press, Oxford, UK.

Goslee SC, Urban DL (2007) The ecodist package for dissimilarity-based analysis of ecological data. *J Stat Softw*, **22**: 1–19.

Hansen TF, Pélabon C, Houle D (2011) Heritability is not evolvability. *Evol Biol*, **38**: 258.

Heidelberger P, Welch PD (1981) A spectral method for confidence interval generation and run length control in simulations. *Commun ACM*, **24**: 233–245.

Houle D (1992) Comparing evolvability and variability of quantitative traits. *Genetics*, **130**: 195–204.

Hubisz MJ, Falush D, Stephens M, Pritchard JK (2009) Inferring weak population structure with the assistance of sample group information. *Mol Ecol Resour*, **9**: 1322–1332.

Jakobsson M, Rosenberg NA (2007) CLUMPP: a cluster matching and permutation program for dealing with label switching and multimodality in analysis of population structure. *Bioinformatics*, **23**: 1801–1806.

Karhunen M, Ovaskainen O (2012) Estimating population-level coancestry coefficients by an admixture F model. *Genetics*, **192**: 609–617.

Karhunen M, Ovaskainen O, Herczeg G, Merilä J (2014) Bringing habitat information into statistical tests of local adaptation in quantitative traits: A case study of nine-spined sticklebacks. *Evolution*, **68**: 559–568.

Legendre P, Fortin MJ (2010) Comparison of the mantel test and alternative approaches for detecting complex multivariate relationships in the spatial analysis of genetic data. *Mol Ecol Res*, **10**: 831–844.

Ovaskainen O, Karhunen M, Zheng C, Arias JMC, Merilä J (2011) A new method to uncover signatures of divergent and stabilizing selection in quantitative traits. *Genetics*, **189**: 621–632.

Pritchard JK, Stephens M, Donnelly PJ (2000) Inference of population structure using multilocus genotype data. *Genetics*, **155**: 945–959.